HDV RNA replication is associated with HBV repression and interferon-stimulated genes induction in super-infected hepatocytes

D. Alfaiate, J. Lucifora, N. Abeywickrama-Samarakoon, M. Michelet, B. Testoni, J.C. Cortay, C. Sureau, F. Zoulim, P. Deny, David Durantel

HDV RNA replication is associated with HBV repression and interferon-stimulated genes induction in super-infected hepatocytes

Dulce Alfaiate[1,2], Julie Lucifora[1,2#], Natali Abeywickrama-Samarakoon[1,2,*], Maud Michelet[1,2,*], Barbara Testoni[1,2], Jean-Claude Cortay[1,2], Camille Sureau[4], Fabien Zoulim[1,2,5,6], Paul Dény[1,3#], David Durantel[1,2,5#]

[1] INSERM U1052, CNRS UMR-5286, Cancer Research Center of Lyon (CRCL), Lyon, 69008, France;
[2] University of Lyon, Université Claude-Bernard (UCBL), 69008 Lyon, France;
[3] Université Paris 13/SPC, UFR SMBH, Laboratoire de Bactériologie, Virologie - Hygiène, GHU Paris Seine Saint Denis, Assistance Publique – Hôpitaux de Paris, Bobigny, France;
[4] Institut National de Transfusion Sanguine, Laboratoire de Virologie Moléculaire, 75015 Paris, France;
[5] Laboratoire d'excellence (LabEx), DEVweCAN, 69008 Lyon, France;
[6] Hospices Civils de Lyon (HCL), 69002 Lyon, France.
** contributed equally*
 # co-correspondence

Correspondence:

David Durantel (david.durantel@inserm.fr), Paul Dény (paul.deny@inserm.fr) and Julie Lucifora (julie.lucifora@inserm.fr)

Address: INSERM U1052, 151 cours Albert Thomas, 69003 Lyon, France

Phone: + 33 4 72 68 19 70; Fax: +33 4 72 68 19 71; mobile +33 6 66 89 19 02

Manuscript information:

Electronic word count: 5426

Number of figures: 8

Number of supplementary files: 1 table and 8 figures

List of abbreviations:

ADAR, adenosine deaminase acting on RNA; aa, amino acid; cccDNA, circular covalently closed DNA; CHD, chronic hepatitis delta; dHepaRG, differentiated HepaRG;

HBV, hepatitis B virus; HDV, hepatitis D virus; HDAg, Hepatitis delta antigen; HIV, human immunodeficiency virus; hNTCP, human sodium taurocholate cotransporting polypeptide; IFN, interferon; ISG, interferon stimulated genes; LR-β lymphotoxin receptor-β; MOI, multiplicity of infection; n.s., non-significant; PAMP, pathogen-associated molecular pattern; pgRNA, pregenomic RNA; PHH, primary human hepatocytes; p.i., post-infection; PRR, pathogen recognition receptor; PEG, polyethylene glycol; SRB, sulforhodamine B; TLR ,toll-like receptor; VGE, virus genome equivalent; WHV, woodchuck hepatitis virus.

Running title

HDV/HBV interplay in innate immune-competent hepatocytes

Key Words:

Hepatitis D virus; hepatitis B virus; viral interference; IFN response; Interferon stimulated genes

Conflict of interest:

No conflict of interest to declare on this work.

Financial support:

Dulce Alfaiate was supported by grants from Fundação Calouste Gulbenkian and Fundação para a Ciência e a Tecnologia. DD, JL, FZ, and PD were supported by grants from ANRS (French national agency for research on AIDS and viral hepatitis; several grants from CSS4), FINOVI (Foundation for innovation in infectiology; project call n°#4), and by INSERM core grants. PD was supported by an INSERM Interface contract. DD and FZ were also supported by FRM (Foundation for medical research; DEQ20110421327), and DEVweCAN LABEX (ANR-10-LABX-0061) of the “Université de Lyon”, within the program "Investissements d'Avenir" (ANR-11-IDEX-0007) operated by the French National Research Agency (ANR).

Acknowledgements

The authors would like to thank Dr Alan Kay for the kind gift of anti-HDAg antibodies and Dr Stephen Urban for the gift of Myrcludex® and the HepG2 hNTCP cell line.

Author’s contributions:

- Study concept and design: DA, JL, FZ, PD and DD
- Acquisition of data: DA, MM, NAS, JL
- Analysis and interpretation of data: DA, JL, PD and DD
- Writing of the manuscript: DA, CS, FZ, JL, PD and DD
- Statistical analysis: DA, BT
- Technical or material support: JCC and CS

HIGHLIGHTS

- A model of super-infection with HDV on HBV-infected hepatocytes was established;
- HDV infection induces a strong IFN response in these immune-competent hepatocytes;
- In this model, HDV infection is associated with HBV inhibition, thus access to recapitulating *in vivo* viral interference;
- This super infection model is also suitable for the evaluation of novel drugs/antivirals, including immune-modulators.

ABSTRACT

Hepatitis D virus (HDV) super-infection of Hepatitis B virus (HBV)-infected patients is the most aggressive form of viral hepatitis. HDV infection is not susceptible to direct anti-HBV drugs, and only suboptimal antiviral responses are obtained with interferon (IFN)-alpha-based therapy. To get insights on HDV replication and interplay with HBV in physiologically relevant hepatocytes, differentiated HepaRG (dHepaRG) cells, previously infected or not with HBV, were infected with HDV, and viral markers were extensively analyzed. Innate and IFN responses to HDV were monitored by measuring pro-inflammatory and interferon-stimulated gene (ISG) expression. Both mono- and super-infected dHepaRG cells supported a strong HDV intracellular replication, which was accompanied by a strong secretion of infectious HDV virions only in the super-infection setting and despite the low number of co-infected cells. Upon HDV super-infection, HBV replication markers including HBeAg, total HBV-DNA and pregenomic RNA were significantly decreased, confirming the interference of HDV on HBV. Yet, no decrease of circular covalently closed HBV DNA (cccDNA) and HBsAg levels was evidenced. At the peak of HDV-RNA accumulation and onset of interference on HBV replication, a strong type-I IFN response was observed, with interferon stimulated genes, *RSAD2* (Viperin) and *IFI78* (MxA) being highly induced. We established a cellular model to characterize in more detail the direct interference of HBV and HDV, and the indirect interplay between the two viruses via innate immune responses. This model will be instrumental to assess molecular and immunological mechanisms of this viral interference.

Introduction

Chronic hepatitis delta (CHD) affects 15-20 million people worldwide (5-10% of the hepatitis B virus (HBV)-infected patients) (1). It is considered to be the most aggressive form of chronic viral hepatitis, with an accelerated progression towards fibrosis and cirrhosis and an increased risk of liver disease decompensation, hepatocellular carcinoma and premature death (2). Pegylated-alpha interferon (Peg-αIFN) remains the sole therapeutic option for these patients, leading to a low virological response rate (< 30%) at 24 weeks post-treatment and high rate (>50%) of late relapse (3). The overall long-term sustained virologic response (SVR) rate is therefore very low in the clinical trial setting, and is even lower in the "real-life" clinical management (4). HBV-reverse transcriptase inhibitors have no effect on hepatitis D virus (HDV) replication. The pipeline of investigational drugs against HDV infection remains limited due to the fact that i) HDV does not encode enzymatic activities and uses cell DNA-dependent RNA polymerases (particularly RNA pol II) for its replication, ii) there are remaining gaps in the knowledge of the viral life-cycle, and iiii) no appropriate *in vitro* model of this satellite co- or super-infection exists to screen antiviral drugs. Amongst few others, Myrcludex (a viral entry inhibitors) and farnesyl transferase (i.e. Lonafarnib) inhibitors are in early clinical trial evaluation (5, 6).

HDV is a subviral agent satellite of HBV, and its genome, the smallest known among mammalian viruses, has similarities to plant viroids. To ensure propagation, HDV relies on HBV, as HDV ribonucleoproteins are surrounded by HBV envelope-embedded glycoproteins. Furthermore, HDV entry into human hepatocytes is mediated through the large HBV envelope protein (L-HBsAg) interaction with the recently discovered cell

surface HBV receptor, *i.e.* the human sodium taurocholate cotransporting polypeptide (hNTCP) (7).

HDV genome is a single-stranded circular RNA of ~1680 bp, with high intra-molecular base pairing, allowing a rod-like structure folding. Its complementary 'antigenomic' strand encompasses the *SHD* gene that codes a single protein, the small, 24 kDa, HD protein (S-HDAg), which is essential for HDV RNA replication. At a later phase of the HDV replication cycle, *SHD* stop codon editing, catalyzed by Adenosine Deaminase acting on RNA-1 (ADAR-1), leads to the synthesis of a 19-20 amino-acid (aa) carboxy-terminal extended isoform of HDAg; this large, 27kDa, protein (L-HDAg), thwarts HDV RNA replication and, in its farnesylated form, is involved in particle assembly (8, 9).

Both clinical and experimental data support the existence of viral interference between HDV and HBV. In the clinical setting, most patients infected with both HBV and HDV feature a pattern of HDV dominance, with a significant decrease in HBV-DNA viral load, when compared to mono-infected patients (10–12). Moreover, studies on liver biopsies from chronically HDV-infected patients have shown a decreased level of HBV replicative intermediates in the liver (13). Finally, this negative interference has been confirmed *in vivo,* in super-infection conditions, using HBV-infected chimpanzees, woodchuck hepatitis virus (WHV)-infected woodchucks, and more recently HBV-infected humanized mice (14–17).

To understand the molecular basis of HDV interference on HBV, relevant infection-based *in vitro* models are essential. Viral interference has been observed in Huh7 cells by transfection of DNA vectors expressing HBV and HDV (or either HDAg isoforms) (18). Direct inhibition of HBV enhancer-1 and activation of *MxA* gene, an interferon-stimulated gene (ISG) known to suppress HBV replication, have been documented in the same cell

line (19). However, transfection models with cDNAs expressing HDV genome have limitations and protein overexpression may lead to inaccurate assumptions. To explore HBV/HDV interference, the access to a cell culture model featuring both cccDNA formation and a competent innate immunity would be instrumental. Until recently, the knowledge on innate immune response related to HDV infection remained scarce. After *in vitro* studies suggesting a modulation of the IFN response (20, 21), recent data from mouse models (both the humanized uPA-SCID and the hNTCP transgenic mice) revealed a strong induction of the intra-hepatocyte ISG expression (22, 23). Further knowledge on the interactions between HDV and the innate immune system could be invaluable to get insights on the interplay between HDV and its helper, as well as to identify novel therapeutic strategies.

The aim of this study was to establish a novel cellular model of HDV super-infection, and characterize HBV/HDV interactions via direct viral interference mechanisms or through hepatocyte innate immune response to infection. This model could furthermore allow an evaluation of novel drugs on HDV replication. Using the differentiated HepaRG (dHepaRG) cells, which are immune-competent (24), we confirmed an efficient suppression of HBV replication (i.e. inhibition of intracellular HBV RNA and DNA accumulation, as well as HBeAg secretion), with no detectable effect on cccDNA nor HBsAg expression, and showed that HDV infection is associated with induction of ISGs, but not with induction of NF-kappaB regulated genes. Finally, we demonstrate the usefulness of this model with respect to antiviral discovery, by studying the antiviral activity of interferon alpha, specific anti-HBV and investigational specific anti-HDV drugs.

Material and Methods

Production of HBV and HDV virions

High-titer HBV particles were retrieved from HepG2.2.15 cells supernatant as previously described (25). HDV particles were produced by Huh7 cotransfection of a trimer HDV-1 prototype replication-competent plasmid (pSVLD3) and an HBsAg-encoding plasmid (pT7HB2.7) according to Sureau et al. (26) (see also **Sup. Fig. 1**). Both HBV and HDV supernatants were concentrated with 8% PEG 8000 (Sigma-Aldrich). All virus preparations were tested for the absence of endotoxin (Lonza).

Cell culture and infection

The human liver progenitor HepaRG cells were cultured, differentiated using DMSO and infected using PEG4% overnight with either HBV or HDV as previously described (24, 25, 27). For super-infection experiments, cells already infected with HBV for 6 days (100 viral genome equivalents [vge]/cell, unless otherwise indicated) were exposed to HDV overnight (100 vge/cell, unless otherwise specified). Primary human hepatocytes (PHH) were isolated and infected as previously reported (25, 26). HepG2-NTCP were kindly provided by Dr Stephan Urban (Univ. Heidelberg, Germany); there were cultivated in 10%-FCS supplemented DMEM (4.5 g/L glucose) without DMSO until confluency and with 2% DMSO after and infected as for HepaRG.

Nucleic acid quantification: qPCR, RT-qPCR and Northern Blot

For HBV titration, DNA was extracted with the QiAmp Ultrasens Virus kit (Qiagen) and submitted to qPCR. HDV was titrated by qRT-PCR after RNA extraction with the NucleoSpin RNA Virus kit (Macherey-Nagel) and digestion with DNAse I (Life Technologies) 1h at 37°C, followed by 20 min at 70ºC, to eliminate residual plasmid DNA.

198 Supernatants from infected-dHepaRG cells were used for viral particle RNA and DNA
199 quantification. In order to remove free nucleic acid, clarified supernatants were submitted
200 to DNAse and RNAse digestion (Roche), followed by overnight precipitation with 8%
201 PEG 8000 (Sigma-Aldrich). After centrifugation, pellets were suspended in PBS 1X and
202 nucleic acids were extracted with the Nucleospin 96 Virus kit (Macherey Nagel). The
203 resultant nucleic acids were quantified using qPCR and RT-qPCR for HBV and HDV,
204 respectively.

205 For HBV intracellular total DNA quantification, DNA extraction was performed using the
206 Master Pure Complete DNA and RNA extraction kit (Epicentre), or the Nucleospin 96
207 tissue kit (Macherey Nagel). Intracellular total RNA was extracted with the NucleoSpin
208 RNA kit (Macherey Nagel), which includes a DNAse digestion step.

209 All primers and probes are listed in **Supplementary Table 1**. HDV quantification was
210 performed by one-step RT-qPCR (Express One-Step SYBR Greener, Life Technologies)
211 using the primers described by Scholtès & colleagues (28), and the following cycling
212 conditions: 50°C for 20 min (retro-transcription - RT), 95°C for 5 min and then 40 cycles
213 of 95°C for 30 s, 60°C for 20 s, and 72°C for 20 s. PCR was run in the Roche LightCycler
214 480. Serial dilution of quantified full length HDV-1 RNA (obtained from *in vitro*
215 transcription of a pCDNA-3-derived plasmid containing a monomeric full length HDV-1
216 cDNA insert) was used as a quantification standard (**Sup. Fig. 2**).

217 HBV DNA/RNA and innate immune gene expression were performed as previously
218 described (25). For cccDNA quantification, total DNA was submitted to digestion with
219 plasmid-safe DNAse (Epicentre) for 4hours at 37ºC, followed by 30 minutes of heat
220 inactivation. Quantification was performed by FRET-based qPCR as previously described
221 (29). Beta globin was used as a house-keeping gene. For all intracellular gene

222 expression analysis, the comparative cycle threshold (Ct) method was applied and
223 results displayed as a ratio, to a control sample (described for each experiment) (30).

224 Northern blot for HDV and HBV RNA detection was essentially performed as previously
225 described (26, 31). Briefly, purified RNA was denatured at 50°C for one hour with glyoxal
226 (Life Technologies), subjected to electrophoresis through a phosphate 1.2% agarose gel
227 and transferred to a nylon membrane (Amersham N+, GE). Membrane-bound RNA was
228 hybridized to 32P-labeled full HDV genome or DIG-labeled HBV-specific probes.
229 Quantitative analysis of HDV RNA was achieved by phosphorimager scanning (Typhoon
230 Fla 9500, GE); 18S and/or 28S rRNA quantification was used as loading control.
231 Quantitative analysis of HBV RNAs was achieved using “ImageLab software” (Bio-Rad).

232

233 ***Elisa, immunofluorescence and western blotting***

234 Commercial immunoassay kits (Autobio Diagnostics Co., China) were used for HBsAg
235 and HBeAg quantification in the cell culture supernatant. Results are presented as a ratio
236 to a control sample, described for each experiment. Cut-offs for these ELISA were 1
237 NCU/mL (i.e. 1 NCU ≈ 13 ng) for HBeAg and 2.5 ng/mL for HBsAg. Human IP-10
238 cytokines were detected in the supernatants using the DuoSet® ELISA kit according to
239 the manufacturer (R&D Systems). Analysis of Secreted Type I Interferon was performed
240 as described previously (24).

241

242 To perform immunofluorescence, cells were fixated with paraformaldehyde 4% and
243 permeabilized by Triton 0.3%. Labeling was done using the following antibodies: HBcAg
244 – monoclonal mouse antibody from Abcam (Ab-8637 – 1/200 dilution); HDAg – polyclonal

in-house rabbit antibody (kind gift from Alan Campbell Kay; 1/200 dilution). Secondary labeling was performed with Alexa Fluor fluorescent antibodies (wavelengths 555 and 488) and cell nuclei were stained with 4.6-diamidino-2-phenylindole (DAPI). All images were obtained by epifluorescence microscopy (Nikon eclipse TE2000-E; Nikon) and processed with ImageJ software. Labeling was quantified by a combination of automatic nuclei counting provided by the software and manual counting of labeled cells. Displayed results correspond to the average of at least three fields (200x magnification).

For Western blots, cell lysis was performed with M-PER reagent (Pierce) in the presence of protease inhibitors. Western blots were performed with standard procedures using in-house polyclonal rabbit anti-HDAg antibodies and anti-tubulin mouse monoclonal antibody (Sigma Aldrich). Detection was performed with Gel Doc XR+ System (BioRad) and images were analyzed with ImageJ software

Antiviral treatment

IFNα (Roche, used at 1000 UI/mL) , tenofovir (Gilead Sciences, used at 10 μM), the farnesylation inhibitor FTI-277 (Sigma Aldrich, used at 10 μM) and Myrcludex® (Kind gift of Dr. Stephan Urban, used at 100 nM) were evaluated of their antiviral effect on an established HDV infection. dHepaRG cells were infected with HBV and super-infected with HDV as previously described and treated at days 3 and 7 and 11 post-HDV infection. Myrcludex® was further evaluated for its effect on HDV entry, by treatment 2 hours before and during HDV inoculation. For all conditions, at day 14 post-HDV infection, supernatants were collected for cytotoxicity evaluation, ELISA and viral nucleic acid extraction and cells were lysed for RNA extraction.

Cell viability and cytotoxicity evaluation

Apolipoprotein B was quantified in cell culture supernatants using the total human Apolipoprotein B ELISA assay (Alerchek), according to the manufacturer's recommendations. Lactate deshydrogenase release was quantified by colorimetric assay (CytoTox 96® Non-Radioactive Cytotoxicity Assay, Promega), according to the manufacturer's protocol. Neutral red uptake assay and Sulforhodamine staining to estimate cell viability/cytotoxicity were performed as previously described (38). To functionally assess the cytotoxic effect of HDV, HDV-infected dHepaRG cells were treated with the apoptosis inhibitor QVD-OPH (Sigma-Aldrich) for 12 days. As a control, dHepaRG were treated with different concentration of the apoptosis inducer Staurosporine (Sigma-Aldrich) for 16h in combination with different concentration of QVD-OPH.

Statistical analysis

Results were computed with Microsoft Office Excel and Prisma Graph Pad softwares. Sample groups were first evaluated for the presence of outliers with Dixon test. Statistical analysis was subsequently performed with Mann-Whitney test for single comparisons and Kruskal-Wallis test with Dunns correction for multiple comparisons. The *p*-values are represented according to the following convention: $p>0.05$ (non-significant, n.s); $p<0.05$ (*); $p<0.01$ (**); $p<0.001$(***).

Results

In a mono-infection setting, dHepaRG cells support a strong, yet transient, HDV replication, associated with a strong expression of ISGs

To assess the conditions of HDV inoculation, dHepaRG cells were either mock-infected or infected with HDV at multiplicities of infection (MOI) ranging from 1 to 500 vge/cell. At day-6 post-infection (p.i.), intracellular HDV RNA could be detected by RT-qPCR from the lowest MOI tested (1 vge/cell), with a linear increase up to 50 vge/cell, reaching a plateau for higher MOIs, up to 500 vge/cell (**Fig. 1A**). Northern blot analysis confirmed RT-qPCR findings and, using a genomic sense probe, indicated *de novo* formation of HDV replicative antigenomic RNA through the initiation of a replicative cycle (**Fig 1B**). This was further confirmed in western blot and IF analyses, showing a plateau of HDV protein expression for MOIs higher than 100 vge/cell and a number of infected cells of no more than 5% of the monolayer (**Fig. 1C and S3**). Importantly, the level of HDV replication in dHepaRG was as high as that observed in HepG2-NTCP cells (40), but 10x lower than that obtained in infected PHH (**Fig. S4**). For the experiments performed later, HDV MOIs of 10 or 100 vge/cell were mainly used for an optimal viral stock management.

To get insights on infection kinetics, dHepaRG cells were infected with HDV and total RNA and proteins were collected sequentially. As a negative control, cells were treated with the entry inhibitor Myrcludex®, from 2 hours before infection up to the end of viral inoculation, as shown in **Fig. 2A**. A steep rise in HDV intracellular RNA accumulation was detected from day 2 p.i. by RT-qPCR, reaching a peak at day 6 and a subsequent decrease (**Fig. 2B and 2C**). At later time point p.i., HDV RNA remained detectable (**Fig. 2A and 2B)**, indicating a residual accumulation of replicative intermediates and/or a low replication persistence. As expected, no significant increase in HDV intracellular RNA

311 occurred in the Myrcludex®-treated control (**Fig. 2**), highly suggesting that the replication
312 detected in the assay occurred after hNTCP receptor-mediated specific entry process.
313 Increase in HDV RNA levels was associated with an increase in the expression of HDAg
314 (**Fig. 2C and S3**), with both forms (S-HDAg and L-HDAg) being clearly detectable from
315 day 3 p.i. (**Fig. 2C**). The pattern of expression was slightly delayed as compared to HDV
316 RNA, but followed the same bell-shaped curve. At later time points both HDAg isoform
317 signals decreased but remained detectable (**Fig. 2C and S3**). A very slight impairment of
318 hepatocyte viability was associated with HDV infection, as documented by levels of
319 secreted ApoB throughout time, neutral-red staining, and sulforhodamine assays (**Fig.**
320 **S6A, S6B and S6C**). However this weakly measurable toxicity did not parallel the kinetic
321 of replication of HDV, as it was constant over time. Moreover, the use of an apoptosis
322 inhibitor (i.e. QVD-OPH) did not modify the level of HDV replication, therefore confirming
323 that HDV do not induce a specific death of infected dHepaRG cells (**Fig. S6D and S6E**).

324 In contrast to hepatoma cells, dHepaRG cells express functional innate immune sensors,
325 namely pathogen recognition receptors (PRRs), and, therefore may be relevant to study
326 antiviral response in hepatocytes (24). We aimed to decipher IFN response to HDV
327 infection in this model. Upon HDV mono-infection, increased expression of several
328 representative *ISGs* could be detected. Interestingly, *ISGs* expression peaked at day-6
329 p.i. and correlated with HDV RNA replication kinetics (**Fig. 3A**). No *ISGs'* induction
330 occurred in the presence of Myrcludex®, excluding a non-specific stimulation by the viral
331 inoculum. Furthermore, no induction was detected during the first 3 days p.i., which may
332 suggest that the IFN response matched HDV RNA replication and HDV RNA neo-
333 synthesis, rather than the incoming viral RNA material. In comparison to non-infected
334 cells, highest expressions were detected for *RSAD2* (i.e. *VIPERIN*; mean fold change
335 289) and *IFI78* (i.e. *MXA*; mean fold change 143,2). Other evaluated genes included

ISG15 (mean fold change 36,2), *OAS1* (mean fold change 21,2), *DDX58* (i.e. *RIGI*; mean fold change 20,7), *MDA5* (mean fold change 9) and *IFN-β* (mean fold change 4,4). For all studied time points, non-significant and less than 2 fold differences in expression were found respectively for *IFN-α* and *IL-6* between HDV infected cells and mock or Myrcludex® treated controls. In addition, we observed an increased secretion of IP-10 and type-I IFN that paralleled the increase of HDV RNA observed with the different amounts of HDV particles used for infection (**Fig. 3B**).

During super-infection, secretion of infectious HDV particles demonstrates the existence of HBV/HDV co-infected cells.

To set up the super-infection model, dHepaRG cells were first inoculated with HBV (100 or 500 vge/cell), and, at the plateau of HBV replication (i.e. day-6) (32), cells were inoculated with HDV. In this setting, three infected cell populations could be identified, upon labeling with anti-HBcAg and anti-HDAg antibodies: HBcAg positive/HDAg negative cells, HBcAg negative/HDAg positive cells and HBcAg positive/HDAg positive cells (**Fig. 4A**). This suggested that cells were either mono-infected by either HBV or HDV, or by both viruses, respectively. The same observation was obtained when HBsAg immunostaining was used instead of HBcAg labeling (**data not shown**). The proportion of infected cells expressing either antigen remained below 5% for either HBV or HDV markers, whereas co-labeling occurred in approximately 1-2% of the total dHepaRG cells.

Interestingly, despite the low number of detectable co-labeled cells, quantification of HDV RNA reached $1.3x10^7$ vge/mL in the supernatant of HBV-HDV super-infected cells for the

best condition. This result was obtained without detectable cell toxicity (**data not shown**), suggesting the secretion of viral particles. As expected, HDV intracellular RNA levels increased significantly with HDV MOI, but non-significantly with HBV MOI (**Fig. 4B**), whereas HDV secretion was proportional to both HDV and HBV MOIs (**Fig. 4C**). Of note, infections of HepG2-NTCP cells with concentrated HDV particles secreted from our super-infection experiments (called HDV-2P, for second passage) were as efficient as primary HDV inoculum (using equivalent MOI). This was demonstrated both by intracellular HDV RNA quantification and HDAg IF staining (**Fig. 4D**). Despite the low number of HBcAg/HDAg-positive cells, and likely due to the high efficiency of HDV-replication per cell (33), in the dHepaRG HBV/HDV super-infection setting, supernatant RNA associated from infectious HDV particles could be easily quantified, demonstrating that some dHepaRG cells can be infected by both viruses and are hence a suitable model for the evaluation of HDV-HBV interactions and the selection of drug resistant HDV variants.

In HBV-infected cells, HDV super-infection is associated with a MOI-dependent induction of ISGs and decreased HBV replication

The expression of innate immune related genes was evaluated at day-15 post-HBV infection (day-9 post-HDV infection). As previously determined (34), HBV alone did not induce any innate gene expression at this time point (**Fig. 5**). In contrast, HDV infection was clearly associated with a strong induction of all studied *ISGs*, which was HDV MOI-dependent but HBV-independent. Consistent with HDV mono-infection, super-infection, induced preferentially *RSAD2* and *MXA*, with a respective 83.5 and a 48.6 fold increased gene expression (at HBV 100 vge/mL and HDV 100 vge/mL). Finally, no induction of NF-κB induced genes was identified in HDV infections, as exemplified for *IL-6* (**Fig. 5**), *IL-8*

and *IL-1β* (**data not shown**). Collectively, these data indicate that in dHepaRG cells, HDV infection induces a strong IFN response at the peak of RNA replication, independently of both HBV infection and NF-κB pathway.

To investigate viral interference in the same setting, replication parameters were analyzed at day-15 post-HBV inoculation (9 days post-HDV super-infection). A significant decrease in both HBeAg secretion and intracellular HBV DNA accumulation was observed upon HDV super-infection of HBV-infected cells and the decrease was more pronounced with increasing HDV MOIs (**Fig. 6A and 6E**). Concomitantly, HBV-DNA level decreased in the supernatant when cells were super-infected by HDV (**Fig. 6D**). In such conditions, no reduction of HBsAg was observed (**Fig. 6B**), and no variation of cccDNA levels occurred (as measured by specific qPCR; **Fig. 6C**). Considering HBV MOI condition of 100 vge/cell, the decrease of HBV pgRNA correlated with the HDV MOI (25% reduction for HDV MOI 100 vs HBV mono-infection; $p<0.05$) (**Fig. 6G and 6H**). In contrast, no variation in the amount of total HBV RNA was observed even at high HDV MOI (**Fig. 6F and 6H**).

To further characterize this viral interference, HBeAg and HBsAg secretion were followed throughout time in dHepaRG inoculated, or not, with HBV (100 vge/cells) and superinfected, or not, with HDV (**Fig. 7A and 7B**). Compared to HBV-mono-infected cells, HDV-super-infected cells displayed a significant decrease of HBeAg secretion (34% decrease, $p<0.01$) (**Fig. 7A**). Increasing HDV MOI further inhibited HBeAg secretion (**Fig. 7B and 7C**) and decreased the number of HBcAg positive cells (**Fig. 7C**) suggesting that viral interference was dependent of HDV-MOI. In contrast, there was no significant difference in HBsAg secretion levels between HBV-mono-infected and HDV-super-infected cells (**Fig. 7A and 7B**).

Study of various drugs for their anti-HDV efficiency

In order to further validate this HBV-HDV super-infection model, we aimed to explore the inhibitory effect of different molecules that could interfere with different steps of HBV and HDV life cycles in infected dHepaRG cells. Besides approved compounds such as IFNα and tenofovir di-fumarate (TDF), we also verified the potential action of the entry inhibitor Myrcludex® and lonafarnib, a farnesyl transferase inhibitor (FTI), that have recently entered in phase II clinical trials for chronic HBV/HDV liver disease indication. Doses and treatment schedules were selected based on previously published data (35–38).

As expected, upon treatment with the HBV-polymerase inhibitor tenofovir, a significant decrease was observed in the amount of secreted HBV DNA (70%; p<0,0001), but not in secreted antigens or intracellular RNA levels (**Fig. S7A)**. No effect was documented on HDV replication or viral secretion (**Fig. 8A**). IFNα treatment led to an important reduction of both HBV and HDV replicative parameters (**Fig 8B and S7B**). Unlike the other drugs, IFNα treatment was associated with a significant decrease in Apolipoprotein B secretion (67%; p<0,0001). As no increased LDH release was observed, such finding may be related to hepatocyte de-differentiation rather than cytotoxicity (**Fig. S8**).

Prenylation inhibitors have been shown both *in vitro* and *in vivo* to impact HDV envelopment and secretion without having a direct effect on viral replication. By treating HBV/HDV super-infected cells with FTI-277, we could observe a modest, albeit non-significant, reduction of HDV secretion into the supernatant (40%, p=0,16), which, interestingly, was associated with an increase of intracellular HDV RNA levels (2 fold increase; p<0,05) (**Fig. 8C**). As expected, FTI-277 treatment had no effect on HBV

replicative markers (**Fig. S7C**). Treatment with combinations of IFNα and tenofovir or FTI-277 and IFNα did not evidence a further decrease of neither HBV nor HDV parameters compared to single drug treatments (**Fig. 8D, 8E, S7D and S7E**). In this model, we could also confirm a suppression of HDV entry by Myrcludex® treatment previous and during HDV inoculation, while excluding a post-entry effect on both HBV and HDV replications (**Fig. 8F and S7F**). Overall, these results validate this model for the evaluation of both immune modulatory and direct-acting antiviral compounds acting on both HBV and HDV and at different steps of the viral life cycles.

Discussion

Despite leading to the most severe form of chronic viral hepatitis and infecting 15 to 20 million of HBV-positive people worldwide, HDV remains a neglected pathogen. Getting more fundamental knowledge on HBV/HDV co-infections and viral interference may ultimately translate into the development of much needed new therapeutic strategies against HDV.

One aim of this work was to implement a relevant cell culture model to study this viral interplay, taking into account a subcellular innate immunity component. PHH are considered as the gold standard to perform *in vitro* studies on HBV and by extension on HDV. However, the low accessibility of fresh human liver resections, as well as the quality and variability of individual preparations limit their use. Interestingly, similarly to PHH, and in contrast to widely-used HepG2 and Huh7 cells, HepaRG cells functionally express most of innate immunity sensors (24) and are therefore considered as immune-competent (39). Despite their lower susceptibility to HBV and HDV infection, dHepaRG are the best alternative to PHH cultures to study HBV infection, as a full replication cycle can be obtained without the need of ectopically expressed hNTCP (32). Moreover, cccDNA can be detected in infected HepaRG cells, and has been shown, in a proof of concept study, to be degradable in an APOBEC3A/B-dependent manner by activation of IFN-α or lymphotoxin receptor-β (LR-β) response pathway(s) (29). Therefore, the HepaRG cell line represents a unique model to study the interplay between HBV/HDV and hepatocyte-specific innate immunity, as well as to explore new therapeutic developments. So far, regarding HDV biology, the HepaRG model has mostly been used for studying the entry step (26), its inhibition by Myrcludex®, a drug competing with

462 hNTCP viral attachment (40), thus confirming the relevance of this cellular receptor for
463 HDV entry (7).

464 In mono-infection with HDV we found that, as expected, only a small percentage of
465 dHepaRG were infected (< 5% in IF). But in contrast to what seen with HBV (32), the
466 intracellular level of HDV replication was very high, and could be detected even without
467 amplification, by northern blot. Notably, in a super-infection setting, despite the very low
468 proportion of co-infected cells (1-2%), neo-produced infectious HDV particles were titered
469 at 10^7 vge/mL in supernatant, thus reflecting again the very high efficiency of viral RNA
470 replication (33). The rather low proportion of detectable infected cells could be due, at
471 least in part, to cell polarization and accessibility of hNTCP in the basolateral membrane
472 of hepatocytes (41). Interestingly, in both mono-infection and super-infection conditions,
473 HDV replication seemed to decline after a peak of replication at day-6 post inoculation. A
474 similar decrease over time has also been described in mice injected with a HDV cDNA
475 construct, in the chimpanzee experimental model and, more recently, in the hNTCP
476 transgenic mouse model (17, 23, 42). At least two hypotheses might explain such
477 phenotype: the infection is limited in time either by the decrease of available factor
478 needed for replication, such as S-HDAg or some proviral host factors, or by accumulation
479 of inhibitors, such as L-HDAg or cellular negative factor(s). Alternatively, active antiviral
480 innate immune response that was, in our experiments, found temporally related to the
481 peak of RNA accumulation, could also contribute to such inhibition.

482 With respect to the former, it was suggested that, besides mediating virion assembly, L-
483 HDAg could inhibit viral replication, and therefore play crucial role to switch life-cycle from
484 replicative to morphogenetic phase (43). However in our model, L-HDAg may not play
485 this role, as the ratio of S-HDAg and L-HDAg remained constant throughout the kinetics

of HDV RNA replication, and in the super-infection setting, in which HDV virion release is observed, the decline of HDV RNA signals after day-6 p.i. is still observed. Regarding the immune hypothesis, we showed that the induction of some *ISGs* expression occurs at the peak of HDV RNA accumulation, indicating that neo-synthesized HDV-replicative intermediates, rather than inoculum RNA, act as a pathogen-associated molecular pattern (PAMP). Whether the activation of IFN response could lead to the decline of HDV replication after day-6 post infection is still unknown in dHepaRG, but such an hypothesis was not confirmed in the transgenic hNTCP mouse model (23).

Interestingly, in the cellular super-infection setting, we were able to confirm that HDV can interfere with HBV replication. The observations that HDV super-infection is associated with a decrease of HBeAg, HBV virion secretion, intracellular HBV DNA and pgRNA, although not HBsAg, total HBV RNA or cccDNA, are in agreement with what has been described in HDV-infected patients (13). This is part of the originality of this satellite infection that may often overcome its helper replication, while maintaining its budding trans-complementation. A competition for viral egress through the HBsAg secretory pathway is unlikely, as HBsAg is produced in large excess leading to a high proportion of empty subviral particles, and both viruses may not have the same cellular egress pathway (45). Furthermore, this would not account for the specific diminution of the HBV pgRNA that might be due to a modulation of cccDNA transcriptional activity (13, 18). In reporter systems and exogenous expression of HD proteins, direct inhibition of both HBV enhancers, especially by L-HDAg has been previously suggested (19). In a previous pioneer work using Huh7 cell co-transfected by both HBV-expressing plasmid pA3HBV3.8 and pSVLD3 (or pSVL-HDAg), J.C. Wu and co-workers suggested a possible repressive effect on transcription of the 3.5 kb and the 2.1 kb transcripts of HBV by HDV-replication or HDAg coding gene expression (18). But this approach was less

physiological than that based on proper infections. We trust the cellular super-infection model described in this study may therefore further contribute to determine at which step (e.g. cccDNA transcription, viral mRNA export and/or stability), and with which kinetic, the HDV-induced HBV-inhibition may occur.

Another explanation of this viral interference may be linked to the HDV-induced IFN response. Our results indicate that an increase in HDV MOI was associated with a more significant decrease of HBV replicative intermediates and a dose-dependent increase in ISGs expression. Previous works on HBV have shown that type-I IFN response modulates transcriptional regulation of cccDNA, decreasing pgRNA synthesis through modifications in histone acetylation status and recruitment of chromatin modifying enzymes (46). Whether HDV super-infection could induce such an epigenetic negative regulation of cccDNA transcription remains to be further explored.

During HDV infection (with and without a previous infection by HBV), we identified a pattern of gene activation suggesting the induction of an IFN response, without any effect on NF-κB regulated genes. The induction of ISGs expression by HDV is fully in agreement with results obtained in in both the humanized and hNTCP transgenic mice (22, 23). Among the studied ISGs genes that match HDV replication, *RDSA2* was found to be the most activated one. Interestingly, it has been suggested that in the woodchuck hepatitis infection of woodchuck neonates, Viperin was found to be at a higher level in neonates that resolved their infection, than those who progress to chronic carriage (47). Another innate-immune mediated mechanism of HBV repression due to HDV super-infection might be linked to a counteract the inhibition of the *MxA* expression probably linked to the HBV capsid (48–50)

Finally, our results demonstrate that, unlike other cellular models, dHepaRG sequentially infected by HBV and HDV represent a relevant model for the evaluation of antiviral drugs. Nucleos(t)ide analogues, such as tenofovir, while widely used in the setting of chronic hepatitis B, have failed to show a beneficial effect on the treatment of HDV infected patients (51, 52). Our data support these findings, as no effect of tenofovir was observed on either HDV replication or HBsAg secretion. Whereas an antiviral effect of IFNα on HBV replication has been thoroughly studied (35), data obtained in cellular models have been conflicting regarding its mechanism of action on HDV. Indeed, no direct effect of interferon on HDV replication was previously demonstrated (20), and other mechanisms of action have been suggested (53, 54). Our findings, being consistent with a suppression of HDV replication by interferon, in the absence of cytotoxicity, are in line with the data obtained *in vivo*, supporting the notion that dHepaRG cells is a more pertinent model than hepatoma derived cells for the evaluation of immune-modulators. We also aimed to evaluate the effect of some investigational drugs, currently undergoing clinical trials. The HBV/HDV entry inhibition we could observe with Myrcludex® treatment confirmed previous data form other groups (15, 40). Although not reaching statistical significance, we reproduced a trend of decreased HDV secretion inhibition by the prenylation inhibitor FTI-277. The fact that this effect was less pronounced than previously described, may be associated with the small number of co-infected cells in the HepaRG cell model. Interestingly, and unlike previous studies, the treatment with FTI-277 in our model was associated with an increased HDV RNA accumulation in the cells. These results, although unexpected, can be explained i) by a possible abrogation of the inhibitory effect of L-HDAg on HDV replication in the absence of prenylation or ii) a defect in assembly of HDV RNP with HBsAg (55).

In summary, we demonstrated here the usefulness of the HepaRG cell line model for the study of HDV infection, in mono- and super-infection settings and could show that a robust HDV replication occurs in these cells and is associated with a strong induction of ISG expression. Moreover, upon HDV-super-infection of HBV-infected cells, HDV/HBV viral interference contributing to lowering HBV expression and the production of infectious HDV particles could be confirmed.

References

1. Hughes SA, Wedemeyer H, Harrison PM. 2011. Hepatitis delta virus. Lancet 378:73–85.
2. Fattovich G, Giustina G, Christensen E, Pantalena M, Zagni I, Realdi G, Schalm SW. 2000. Influence of hepatitis delta virus infection on morbidity and mortality in compensated cirrhosis type B. The European Concerted Action on Viral Hepatitis (Eurohep). Gut 46:420–426.
3. Heidrich B, Yurdaydın C, Kabaçam G, Ratsch BA, Zachou K, Bremer B, Dalekos GN, Erhardt A, Tabak F, Yalcin K, Gürel S, Zeuzem S, Cornberg M, Bock C-T, Manns MP, Wedemeyer H, HIDIT-1 Study Group. 2014. Late HDV RNA relapse after peginterferon alpha-based therapy of chronic hepatitis delta. Hepatol Baltim Md 60:87–97.
4. Yurdaydin C. 2012. Treatment of chronic delta hepatitis. Semin Liver Dis 32:237–244.
5. Koh C, Canini L, Dahari H, Zhao X, Uprichard SL, Haynes-Williams V, Winters MA, Subramanya G, Cooper SL, Pinto P, Wolff EF, Bishop R, Ai Thanda Han M, Cotler SJ, Kleiner DE, Keskin O, Idilman R, Yurdaydin C, Glenn JS, Heller T. 2015. Oral prenylation inhibition with lonafarnib in chronic hepatitis D infection: a proof-of-concept randomised, double-blind, placebo-controlled phase 2A trial. Lancet Infect Dis 15:1167-74.
6. Bogomolov P, Alexandrov A, Voronkova N, Macievich M, Kokina K, Petrachenkova M, Lehr T, Lempp FA, Wedemeyer H, Haag M, Schwab M, Haefeli WE, Blank A, Urban S. 2016. Interim results of a Phase Ib/IIa study of the entry inhibitor myrcludex B in chronic hepatitis D infected patients. J Hepatol 65:490-8.
7. Yan H, Zhong G, Xu G, He W, Jing Z, Gao Z, Huang Y, Qi Y, Peng B, Wang H, Fu L, Song M, Chen P, Gao W, Ren B, Sun Y, Cai T, Feng X, Sui J, Li W. 2012. Sodium taurocholate cotransporting polypeptide is a functional receptor for human hepatitis B and D virus. eLife 13:1:e00049.

8. Lai MMC. 2005. RNA replication without RNA-dependent RNA polymerase: surprises from hepatitis delta virus. J Virol 79:7951–7958.

9. Taylor JM. 2012. Virology of hepatitis D virus. Semin Liver Dis 32:195–200.

10. Schaper M, Rodriguez-Frias F, Jardi R, Tabernero D, Homs M, Ruiz G, Quer J, Esteban R, Buti M. 2010. Quantitative longitudinal evaluations of hepatitis delta virus RNA and hepatitis B virus DNA shows a dynamic, complex replicative profile in chronic hepatitis B and D. J Hepatol 52:658–664.

11. Krogsgaard K, Kryger P, Aldershvile J, Andersson P, Sørensen TI, Nielsen JO. 1987. Delta-infection and suppression of hepatitis B virus replication in chronic HBsAg carriers. Hepatol Baltim Md 7:42–45.

12. Genesca J, Jardi R, Buti M, Vives L, Prat S, Esteban JI, Esteban R, Guardia J. 1987. Hepatitis B virus replication in acute hepatitis B, acute hepatitis B virus-hepatitis delta virus coinfection and acute hepatitis delta superinfection. Hepatol Baltim Md 7:569–572.

13. Pollicino T, Raffa G, Santantonio T, Gaeta GB, Iannello G, Alibrandi A, Squadrito G, Cacciola I, Calvi C, Colucci G, Levrero M, Raimondo G. 2011. Replicative and transcriptional activities of hepatitis B virus in patients coinfected with hepatitis B and hepatitis delta viruses. J Virol 85:432–439.

14. Rizzetto M, Canese MG, Gerin JL, London WT, Sly DL, Purcell RH. 1980. Transmission of the hepatitis B virus-associated delta antigen to chimpanzees. J Infect Dis 141:590–602.

15. Lütgehetmann M, Mancke LV, Volz T, Helbig M, Allweiss L, Bornscheuer T, Pollok JM, Lohse AW, Petersen J, Urban S, Dandri M. 2012. Humanized chimeric uPA mouse model for the study of hepatitis B and D virus interactions and preclinical drug evaluation. Hepatol Baltim Md 55:685–694.

16. Negro F, Korba BE, Forzani B, Baroudy BM, Brown TL, Gerin JL, Ponzetto A. 1989. Hepatitis delta virus (HDV) and woodchuck hepatitis virus (WHV) nucleic acids in tissues of HDV-infected chronic WHV carrier woodchucks. J Virol 63:1612–1618.

17. Sureau C, Taylor J, Chao M, Eichberg JW, Lanford RE. 1989. Cloned hepatitis delta virus cDNA is infectious in the chimpanzee. J Virol 63:4292–4297.

18. Wu JC, Chen PJ, Kuo MY, Lee SD, Chen DS, Ting LP. 1991. Production of hepatitis delta virus and suppression of helper hepatitis B virus in a human hepatoma cell line. J Virol 65:1099–1104.

19. Williams V, Brichler S, Radjef N, Lebon P, Goffard A, Hober D, Fagard R, Kremsdorf D, Dény P, Gordien E. 2009. Hepatitis delta virus proteins repress hepatitis B virus enhancers and activate the alpha/beta interferon-inducible MxA gene. J Gen Virol 90:2759–2767.

20. McNair AN, Cheng D, Monjardino J, Thomas HC, Kerr IM. 1994. Hepatitis delta virus replication in vitro is not affected by interferon-alpha or -gamma despite intact cellular responses to interferon and dsRNA. J Gen Virol 75 (Pt 6):1371–1378.

21. Pugnale P, Pazienza V, Guilloux K, Negro F. 2009. Hepatitis delta virus inhibits alpha interferon signaling. Hepatol Baltim Md 49:398–406.

22. Giersch K, Allweiss L, Volz T, Helbig M, Bierwolf J, Lohse AW, Pollok JM, Petersen J, Dandri M, Lütgehetmann M. 2015. Hepatitis Delta co-infection in humanized mice

leads to pronounced induction of innate immune responses in comparison to HBV mono-infection. J Hepatol 63: 346-53.

23. He W, Ren B, Mao F, Jing Z, Li Y, Liu Y, Peng B, Yan H, Qi Y, Sun Y, Guo J-T, Sui J, Wang F, Li W. 2015. Hepatitis D Virus Infection of Mice Expressing Human Sodium Taurocholate Co-transporting Polypeptide. PLoS Pathog 11:e1004840.

24. Luangsay S, Ait-Goughoulte M, Michelet M, Floriot O, Bonnin M, Gruffaz M, Rivoire M, Fletcher S, Javanbakht H, Lucifora J, Zoulim F, Durantel D. 2015. Expression and Functionality of Toll- and RIG-like receptors in HepaRG Cells. J Hepatol 63:1077-85.

25. Luangsay S, Gruffaz M, Isorce N, Testoni B, Michelet M, Faure-Dupuy S, Ait-Goughoulte M, Romain P, Rivoire M, Javanbakht H, Lucifora J, Durantel D, Zoulim F. 2015. Early Inhibition of Hepatocyte Innate Responses by Hepatitis B Virus. J Hepatol 63:1314-22.

26. Sureau C. 2010. The use of hepatocytes to investigate HDV infection: the HDV/HepaRG model. Methods Mol Biol Clifton NJ 640:463–473.

27. Gripon P, Rumin S, Urban S, Le Seyec J, Glaise D, Cannie I, Guyomard C, Lucas J, Trepo C, Guguen-Guillouzo C. 2002. Infection of a human hepatoma cell line by hepatitis B virus. Proc Natl Acad Sci U S A 99:15655–15660.

28. Scholtes C, Icard V, Amiri M, Chevallier-Queyron P, Trabaud M-A, Ramière C, Zoulim F, André P, Dény P. 2012. Standardized one-step real-time reverse transcription-PCR assay for universal detection and quantification of hepatitis delta virus from clinical samples in the presence of a heterologous internal-control RNA. J Clin Microbiol 50:2126–2128.

29. Werle-Lapostolle B, Bowden S, Locarnini S, Wursthorn K, Petersen J, Lau G, Trepo C, Marcellin P, Goodman Z, Delaney WE, Xiong S, Brosgart CL, Chen S-S, Gibbs CS, Zoulim F. 2004. Persistence of cccDNA during the natural history of chronic hepatitis B and decline during adefovir dipivoxil therapy. Gastroenterology 126:1750–1758.

30. Schmittgen TD, Livak KJ. 2008. Analyzing real-time PCR data by the comparative C(T) method. Nat Protoc 3:1101–1108.

31. Lucifora J, Durantel D, Belloni L, Barraud L, Villet S, Vincent IE, Margeridon-Thermet S, Hantz O, Kay A, Levrero M, Zoulim F. 2008. Initiation of hepatitis B virus genome replication and production of infectious virus following delivery in HepG2 cells by novel recombinant baculovirus vector. J Gen Virol 89:1819–1828.

32. Hantz O, Parent R, Durantel D, Gripon P, Guguen-Guillouzo C, Zoulim F. 2009. Persistence of the hepatitis B virus covalently closed circular DNA in HepaRG human hepatocyte-like cells. J Gen Virol 90:127–135.

33. Chen PJ, Kalpana G, Goldberg J, Mason W, Werner B, Gerin J, Taylor J. 1986. Structure and replication of the genome of the hepatitis delta virus. Proc Natl Acad Sci U S A 83:8774–8778.

34. Luangsay S, Gruffaz M, Isorce N, Testoni B, Michelet M, Faure-Dupuy S, Ait-Goughoulte M, Romain P, Rivoire M, Javanbakht H, Lucifora J, Durantel D, Zoulim F. 2015. Early Inhibition of Hepatocyte Innate Responses by Hepatitis B Virus. J Hepatol.

35. Lucifora J, Xia Y, Reisinger F, Zhang K, Stadler D, Cheng X, Sprinzl MF, Koppensteiner H, Makowska Z, Volz T, Remouchamps C, Chou W-M, Thasler WE, Hüser N, Durantel D, Liang TJ, Münk C, Heim MH, Browning JL, Dejardin E, Dandri M, Schindler M, Heikenwalder M, Protzer U. 2014. Specific and nonhepatotoxic degradation of nuclear hepatitis B virus cccDNA. Science 343:1221–1228.

36. Bordier BB, Marion PL, Ohashi K, Kay MA, Greenberg HB, Casey JL, Glenn JS. 2002. A prenylation inhibitor prevents production of infectious hepatitis delta virus particles. J Virol 76:10465–10472.

37. Ni Y, Lempp FA, Mehrle S, Nkongolo S, Kaufman C, Fälth M, Stindt J, Königer C, Nassal M, Kubitz R, Sültmann H, Urban S. 2014. Hepatitis B and D viruses exploit sodium taurocholate co-transporting polypeptide for species-specific entry into hepatocytes. Gastroenterology 146:1070–1083.

38. Isorce N, Testoni B, Locatelli M, Fresquet J, Rivoire M, Luangsay S, Zoulim F, Durantel D. 2016. Antiviral activity of various interferons and pro-inflammatory cytokines in non-transformed cultured hepatocytes infected with hepatitis B virus. Antiviral Res130:36-45.

39. Maire M, Parent R, Morand A-L, Alotte C, Trépo C, Durantel D, Petit M-A. 2008. Characterization of the double-stranded RNA responses in human liver progenitor cells. Biochem Biophys Res Commun 368:556–562.

40. Ni Y, Lempp FA, Mehrle S, Nkongolo S, Kaufman C, Fälth M, Stindt J, Königer C, Nassal M, Kubitz R, Sültmann H, Urban S. 2014. Hepatitis B and D viruses exploit sodium taurocholate co-transporting polypeptide for species-specific entry into hepatocytes. Gastroenterology 146:1070–1083.

41. Schulze A, Mills K, Weiss TS, Urban S. 2012. Hepatocyte polarization is essential for the productive entry of the hepatitis B virus. Hepatol Baltim Md 55:373–383.

42. Chang J, Sigal LJ, Lerro A, Taylor J. 2001. Replication of the human hepatitis delta virus genome Is initiated in mouse hepatocytes following intravenous injection of naked DNA or RNA sequences. J Virol 75:3469–3473.

43. Modahl LE, Lai MM. 2000. The large delta antigen of hepatitis delta virus potently inhibits genomic but not antigenomic RNA synthesis: a mechanism enabling initiation of viral replication. J Virol 74:7375–7380.

44. Macnaughton TB, Lai MMC. 2002. Large hepatitis delta antigen is not a suppressor of hepatitis delta virus RNA synthesis once RNA replication is established. J Virol 76:9910–9919.

45. Watanabe T, Sorensen EM, Naito A, Schott M, Kim S, Ahlquist P. 2007. Involvement of host cellular multivesicular body functions in hepatitis B virus budding. Proc Natl Acad Sci U S A 104:10205–10210.

46. Belloni L, Allweiss L, Guerrieri F, Pediconi N, Volz T, Pollicino T, Petersen J, Raimondo G, Dandri M, Levrero M. 2012. IFN-α inhibits HBV transcription and replication in cell culture and in humanized mice by targeting the epigenetic regulation of the nuclear cccDNA minichromosome. J Clin Invest 122:529–537.

47. Fletcher SP, Chin DJ, Cheng DT, Ravindran P, Bitter H, Gruenbaum L, Cote PJ, Ma H, Klumpp K, Menne S. 2013. Identification of an intrahepatic transcriptional

724 signature associated with self-limiting infection in the woodchuck model of hepatitis
725 B. Hepatol Baltim Md 57:13–22.

726 48. Rosmorduc O, Sirma H, Soussan P, Gordien E, Lebon P, Horisberger M, Bréchot C,
727 Kremsdorf D. 1999. Inhibition of interferon-inducible MxA protein expression by
728 hepatitis B virus capsid protein. J Gen Virol 80 (Pt 5):1253–1262.

729 49. Fernández M, Quiroga JA, Carreño V. 2003. Hepatitis B virus downregulates the
730 human interferon-inducible MxA promoter through direct interaction of precore/core
731 proteins. J Gen Virol 84:2073–2082.

732 50. Li N, Zhang L, Chen L, Feng W, Xu Y, Chen F, Liu X, Chen Z, Liu W. 2012. MxA
733 inhibits hepatitis B virus replication by interaction with hepatitis B core antigen.
734 Hepatol Baltim Md 56:803–811.

735 51. Wedemeyer H, Yurdaydin C, Ernst S, Caruntu FA, Curescu MG, Yalcin K, Akarca
736 US, Gürel S, Zeuzem S, Erhardt A, Lüth S, Papatheodoridis GV, Keskin O, Port K,
737 Radu M, Celen MK, Ildeman R, Stift J, Heidrich B, Mederacke I, Hardtke S, Koch A,
738 Dienes HP, Manns MP. 2014. Prolonged therapy of hepatitis delta for 96 weeks with
739 pegylated-interferon-α-2a plus tenofovir or placebo does not prevent HDV rna
740 relapse after treatment: the HIDIT-2 study. J Hepatol 60:S2–S3.

741 52. Wedemeyer H, Yurdaydìn C, Dalekos GN, Erhardt A, Çakaloğlu Y, Değertekin H,
742 Gürel S, Zeuzem S, Zachou K, Bozkaya H, Koch A, Bock T, Dienes HP, Manns MP,
743 HIDIT Study Group. 2011. Peginterferon plus adefovir versus either drug alone for
744 hepatitis delta. N Engl J Med 364:322–331.

745 53. Taylor JM, Han Z. 2010. Purinergic receptor functionality is necessary for infection of
746 human hepatocytes by hepatitis delta virus and hepatitis B virus. PloS One
747 5:e15784.

748 54. Hartwig D, Schoeneich L, Greeve J, Schütte C, Dorn I, Kirchner H, Hennig H. 2004.
749 Interferon-alpha stimulation of liver cells enhances hepatitis delta virus RNA editing
750 in early infection. J Hepatol 41:667–672.

751 55. Hwang SB, Lai MM. 1993. Isoprenylation mediates direct protein-protein interactions
752 between hepatitis large delta antigen and hepatitis B virus surface antigen. J Virol
753 67:7659–7662.

754

755

Figure legends

Figure 1. MOI-dependent replication of HDV in dHepaRG cells in mono-infection setting. dHepaRG were infected with HDV at different MOIs (ranging from 1 to 500 vge/cell). At day-6 post-infection, (**A**) levels of intracellular HDV RNA were assessed by RT-qPCR or (**B**) northern blot analyses using a genomic probe for antigenome detection, (**C**) HDAg expression was evidenced by western blot. Data in (**A**) represent the mean +/- SEM of 3 independent experiments. *MOI*, multiplicity of infection; *AG*, antigenome; *L-HDAg*, large hepatitis delta antigen; *S-HDAg*, small hepatitis delta antigen; *n.s.*, non-significant.

Figure 2. Kinetics of HDV mono-infection in dHepaRG cells. dHepaRG cells were infected with HDV at 10 vge/cell and viral parameters were followed over time. As controls, cells were treated or not with Myrcludex® at 100nM for 2h before and during HDV inoculation. At the indicated time, (**A**) levels of intracellular HDV RNA were assessed by RT-qPCR or (**B**) northern blot analyses using a genomic probe for antigenome detection, (**C**) HDAg expression was evaluated by western blot. Data in (**A**) represent the mean +/- SEM of 3 independent experiments. *Myr*, Myrcludex®; *AG*, antigenome; *L-HDAg*, large hepatitis delta antigen; *S-HDAg*, small hepatitis delta antigen.

Figure 3. Kinetics of *IL-6*, *IFNs*, and *ISGs* expression in HDV-infected cells & MOI-dependent secretion of IP10 and type-I IFNs. (A) dHepaRG cells were inoculated with HDV at 10 vge/cell and cells were harvested at different time points post-inoculation. *IL-6*, *type-1 IFNs* and *ISG* expressions were evaluated by RT-qPCR. Controls included

779 mock-infected cells, and cells treated with Myrcludex® at 100nM for 2h before and during
780 HDV inoculation. (**B**) dHepaRG cells were inoculated with HDV at indicated MOIs. Six
781 days later, levels of intracellular HDV RNA were assessed by RT-qPCR and IP10
782 secretion or type I IFN activity were respectively assessed by ELISA or reporter gene
783 assay. Results are presented as ratio to the mock condition at each day and represent
784 the mean +/- SEM of 3 independent experiments each performed in triplicate.

785

786 **Figure 4. HDV super-infection of HBV infected dHepaRG leads to secretion of HDV**
787 **infectious particles.** (**A, B, C**) dHepaRG cells were infected by HBV and super-infected
788 by HDV at day-6 at indicated MOIs. Fourteen days post-HBV inoculation, (**A**) cells were
789 labeled with anti-HBcAg or anti-HDAg antibodies (magnification 600X), (**B**) levels of
790 intracellular or (**C**) secreted HDV RNA were assessed by qRT-PCR. Results are
791 presented as ratio (**B**) to cells co-infected with HBV MOI 100 plus HDV MOI 100 or (**C**) to
792 cells infected with HBV HDV MOI 100 and represent the mean +/- SEM of 2 independent
793 experiments each performed in triplicate. (**D**) HepG2-NTCP cells were inoculated with
794 HDV or concentrated supernatant from HBV/HDV co-infected dHepaRG cells (HDV-2P)
795 at 10 vge/cell. As controls, cells were treated or not with Myrcludex® at 100nM for 2h
796 before and during HDV inoculation. 6 days later, levels of intracellular HDV RNA and
797 HDAg were respectively assessed by qRT-PCR or immunofluorescent staining followed
798 by confocal microscopy analyses. Results are presented as ratio to HDV infected cells
799 and represent the mean +/- SEM of one representative experiment performed in
800 triplicate.

801

Figure 5. ISG induction is also present in a super-infection setting. dHepRG cells were either mock (i.e. 0 vge/mL) or infected with HBV at 100 vge/cell and, 6 days later, super-infected with HDV at 0, 10 or 100 vge/cell. *IL-6*, *type-1 IFNs* and *ISGs* expressions were evaluated by RT-qPCR at day-15 post-HBV infection. Results are presented as ratio to the mock condition at each day and represent the mean +/- SEM of 3 independent experiments each performed in triplicate.

Figure 6. HDV super-infection of HBV-infected cells leads to inhibition of HBV replication. Differentiated HepRG cells were either mock (i.e. 0 vge/mL) or infected with HBV at 100 vge/cell and, 6 days later, super-infected with HDV at 0, 10 or 100 vge/cell. At day-15 post-HBV infection, (**A**) HBeAg and (**B**) HBsAg secretion were assessed by ELISA, (**C)** HBV cccDNA, (**D)** HBV secreted DNA and (**E)** HBV total intracellular DNA were assessed by qPCR whereas (**F, H)** HBV total intracellular RNA or (**G, H)** HBV pre-genomic RNA (pgRNA) were assessed by (**F, G**) RT-qPCR and (**H**) northern blot analyses. Results are presented as ratio to HBV cells infected at MOI 100 and represent the mean +/- SEM of 3 independent experiments each performed in triplicate.

Figure 7. HDV super-infection affects HBeAg, but not HBsAg, secretions and intracellular HBcAg expression. Differentiated HepaRG cells were either mock or infected with HBV at 100 vge/cell for 6 days and either mock- or super-infected with HDV at the indicated MOI. (**A, B**) At the indicated time, HBeAg and HBsAg secretion were assessed by ELISA. (**C**) At day 15 post HBV-infection, HBcAg and HDAg were detected by immunofluorescent specific staining and confocal microscopy analyses.

825

826 **Figure 8. Evaluation of the anti-HDV effect of approved and investigational**
827 **molecules.** Differentiated HepaRG cells were infected with HBV at 100 vge/cell for 6
828 days and super-infected with HDV at the indicated at 10 vge/mL. Three days post HDV
829 infection, cells were treated with (**A**) Tenofovir, (**B**) IFNα, (**C**) FTI-277, (**D**) Tenofovir and
830 IFNα, (**E**) FTI-277 and IFNα for 10 days. (**F**) Cells were treated with Myrcludex B (Myr)
831 either 2 hours before and during HDV inoculation (Pre) or once the infection was
832 established as described for the other drugs. Levels of intracellular (RNAic) or secreted
833 (RNA SN) HDV RNA were assessed by qRT-PCR. Results are presented as ratio to the
834 non treated condition and represent the mean +/- SEM of 6 independent experiments
835 each performed in triplicate.

836

Figure 1.

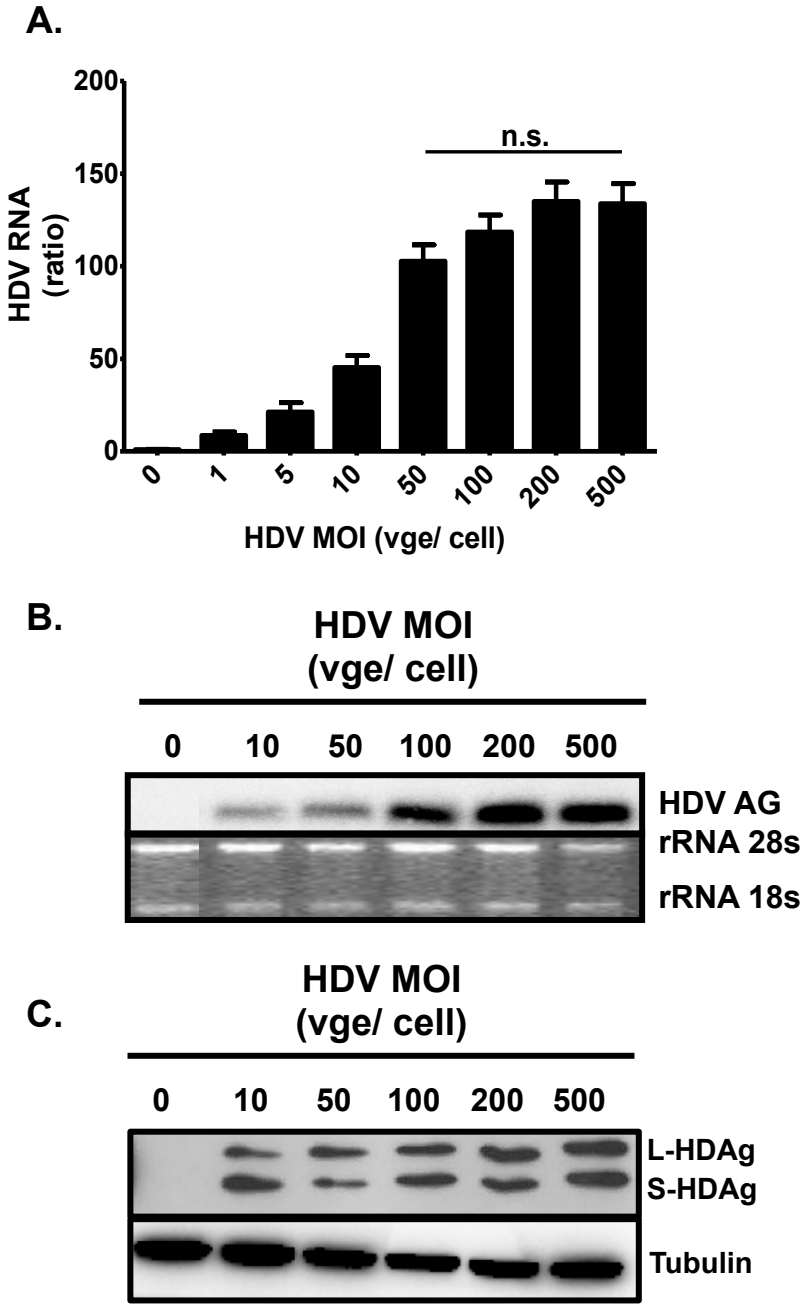
A.
200
150
100
50
0
HDV RNA (ratio)
n.s.
0
1
5
10
50
100
200
500
HDV MOI (vge/ cell)
B.
HDV MOI (vge/ cell)
0
10
50
100
200
500
HDV AG
rRNA 28s
rRNA 18s
C.
HDV MOI (vge/ cell)
0
10
50
100
200
500
L-HDAg
S-HDAg
Tubulin

Figure 2.

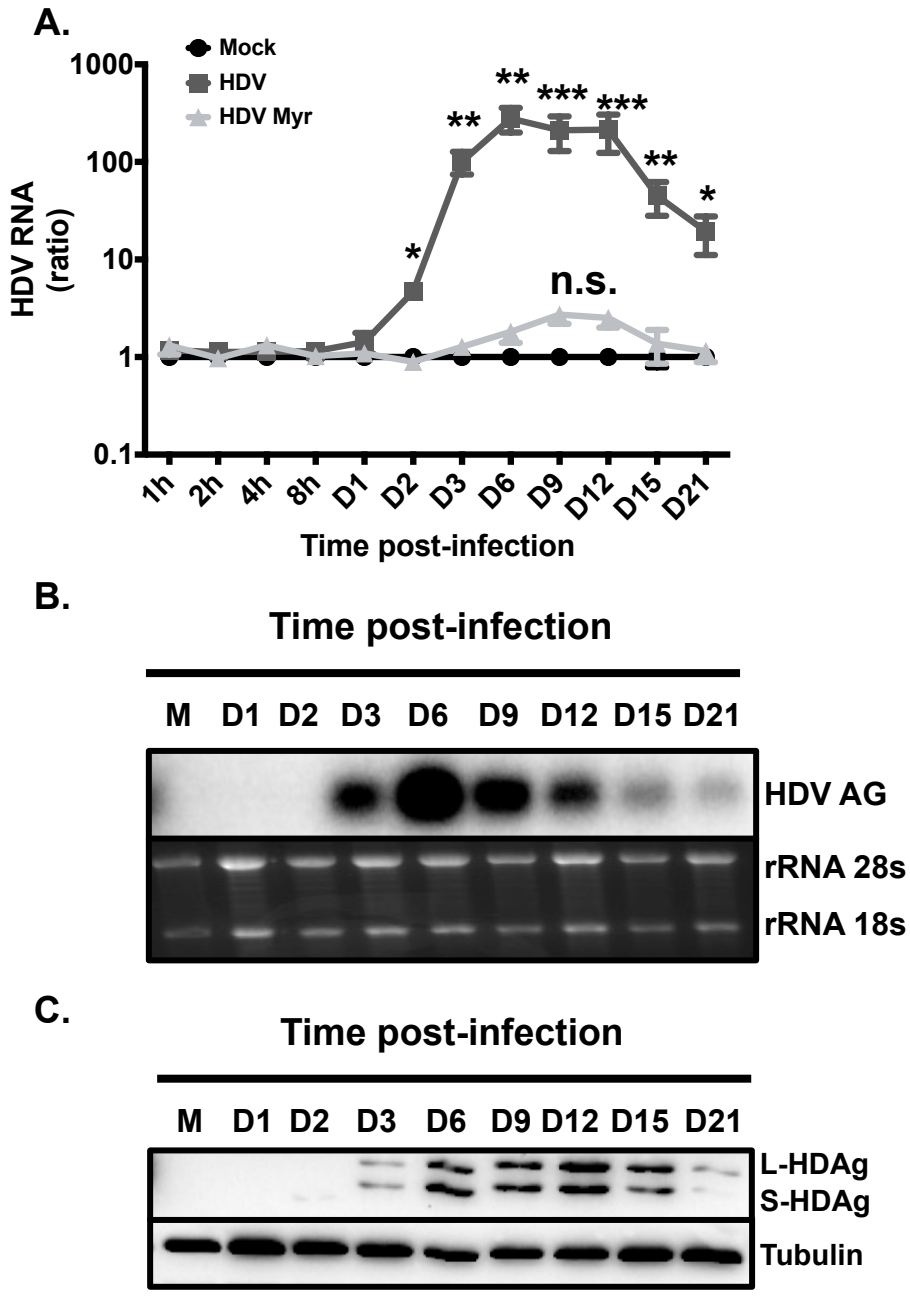
A.
Mock
HDV
HDV Myr
1000
100
10
1
0.1
HDV RNA (ratio)
*
**
**
***
***
**
*
n.s.
1h
2h
4h
8h
D1
D2
D3
D6
D9
D12
D15
D21
Time post-infection
B.
Time post-infection
M
D1
D2
D3
D6
D9
D12
D15
D21
HDV AG
rRNA 28s
rRNA 18s
C.
Time post-infection
M
D1
D2
D3
D6
D9
D12
D15
D21
L-HDAg
S-HDAg
Tubulin

Figure 3.

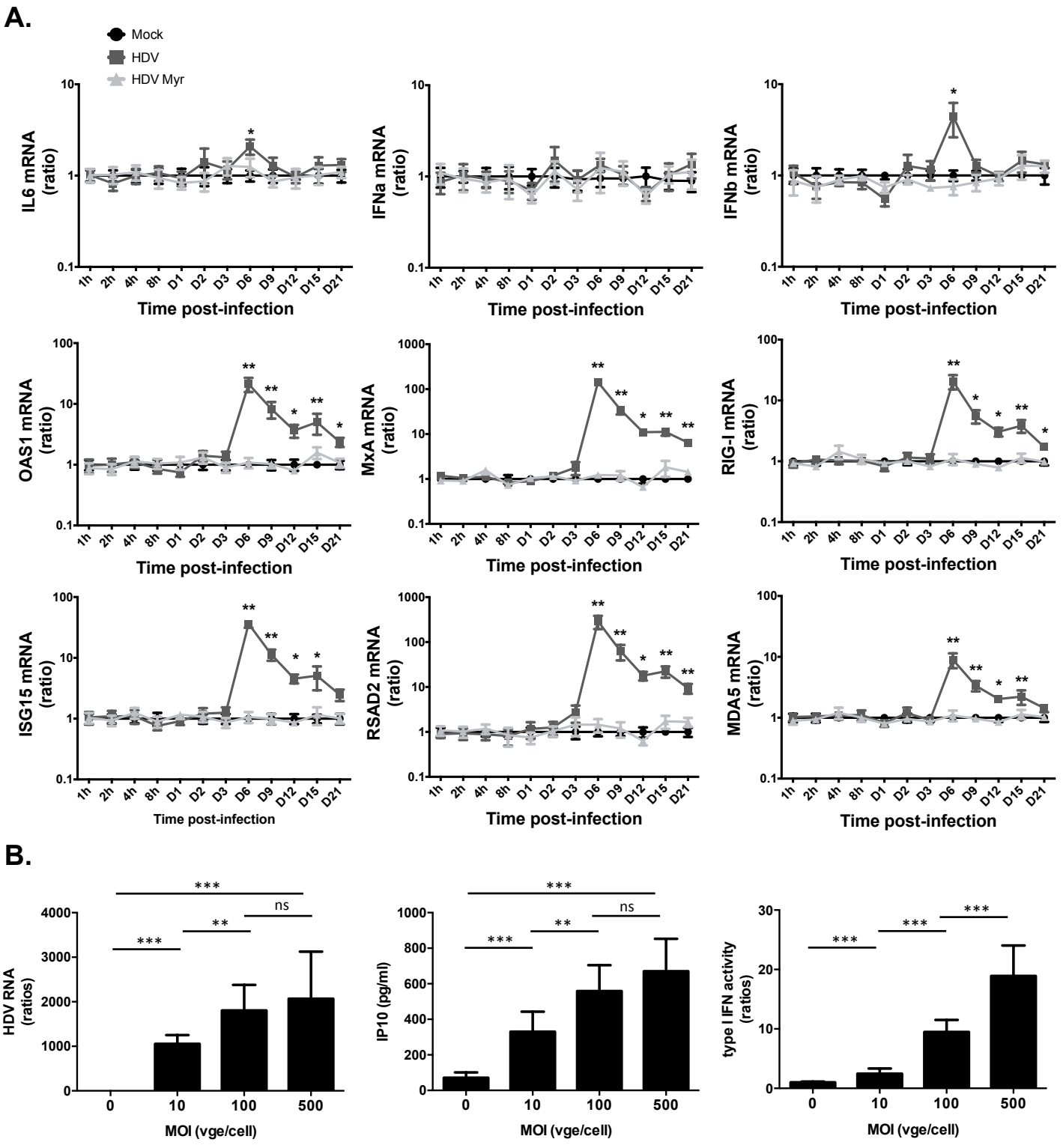
A.
Mock
HDV
HDV Myr
IL6 mRNA (ratio)
IFNa mRNA (ratio)
IFNb mRNA (ratio)
OAS1 mRNA (ratio)
MxA mRNA (ratio)
RIG-I mRNA (ratio)
ISG15 mRNA (ratio)
RSAD2 mRNA (ratio)
MDA5 mRNA (ratio)
Time post-infection
1h 2h 4h 8h D1 D2 D3 D6 D9 D12 D15 D21
B.
HDV RNA (ratios)
IP10 (pg/ml)
type I IFN activity (ratios)
MOI (vge/cell)
0 10 100 500
***
**
*
ns

Figure 4.

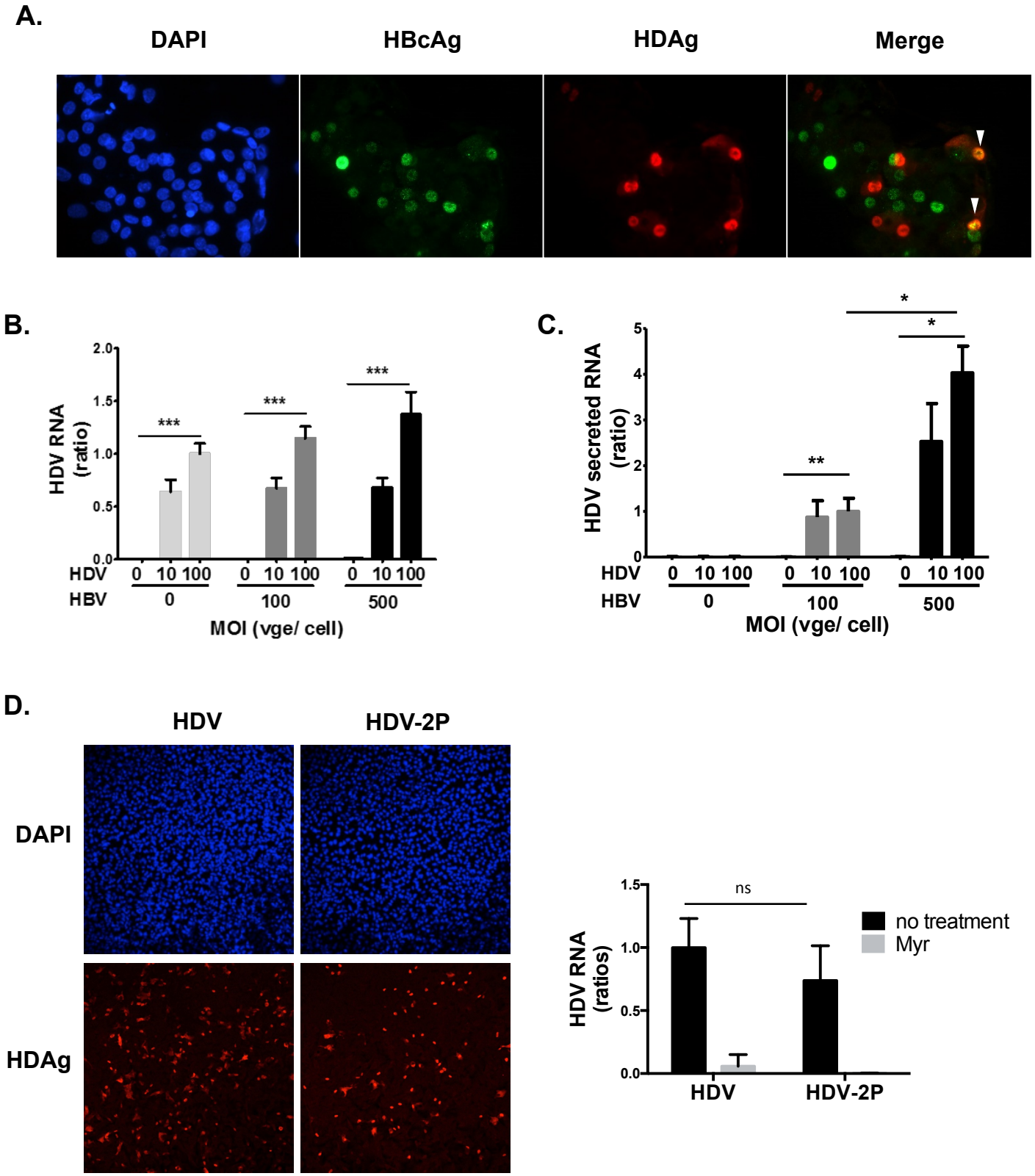
A.
DAPI
HBcAg
HDAg
Merge
B.
HDV RNA (ratio)
2.0
1.5
1.0
0.5
0.0
***
***
***
HDV 0 10 100 0 10 100 0 10 100
HBV 0 100 500
MOI (vge/ cell)
C.
HDV secreted RNA (ratio)
5
4
3
2
1
0
*
*
**
HDV 0 10 100 0 10 100 0 10 100
HBV 0 100 500
MOI (vge/ cell)
D.
HDV
HDV-2P
DAPI
HDAg
HDV RNA (ratios)
1.5
1.0
0.5
0.0
ns
no treatment
Myr
HDV
HDV-2P

Figure 5.

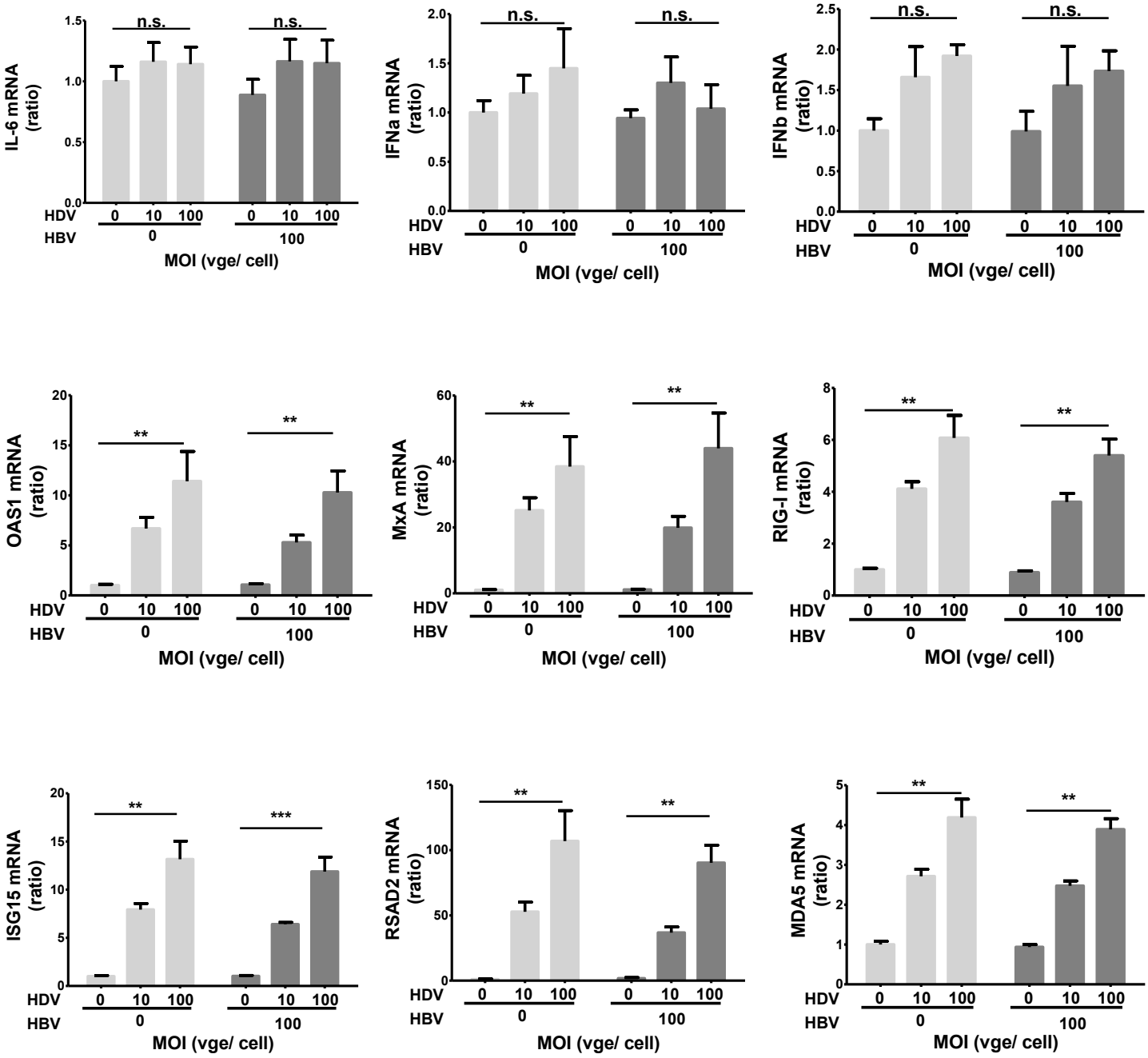
IL-6 mRNA (ratio)
IFNa mRNA (ratio)
IFNb mRNA (ratio)
OAS1 mRNA (ratio)
MxA mRNA (ratio)
RIG-I mRNA (ratio)
ISG15 mRNA (ratio)
RSAD2 mRNA (ratio)
MDA5 mRNA (ratio)
n.s.
**
***
HDV 0 10 100 0 10 100
HBV 0 100
MOI (vge/ cell)

Figure 6.

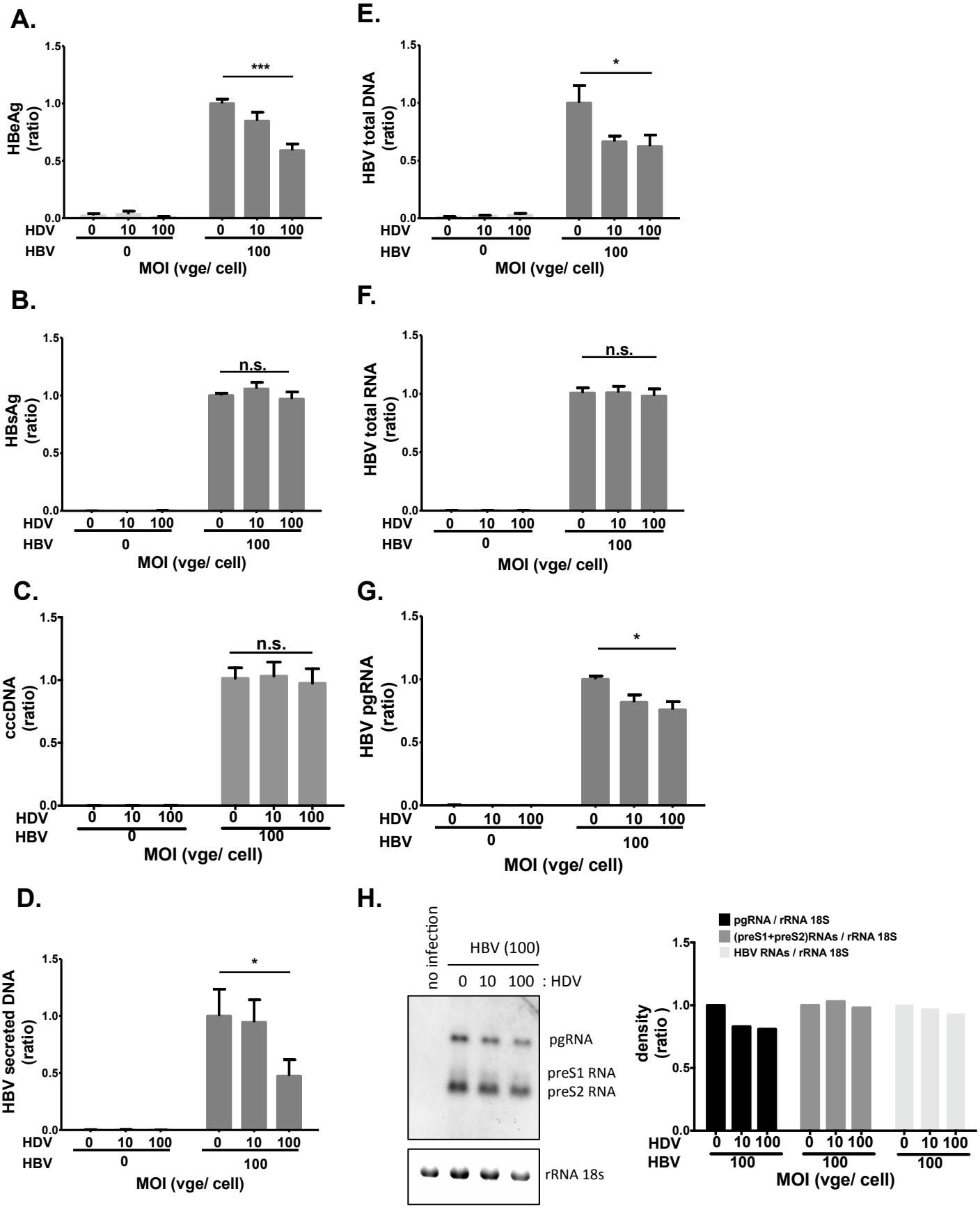
A.
HBeAg (ratio)
***
B.
HBsAg (ratio)
n.s.
C.
cccDNA (ratio)
n.s.
D.
HBV secreted DNA (ratio)
*
E.
HBV total DNA (ratio)
*
F.
HBV total RNA (ratio)
n.s.
G.
HBV pgRNA (ratio)
*
HDV 0 10 100 0 10 100
HBV 0 100
MOI (vge/ cell)
H.
no infection
HBV (100)
0 10 100 : HDV
pgRNA
preS1 RNA
preS2 RNA
rRNA 18s
pgRNA / rRNA 18S
(preS1+preS2)RNAs / rRNA 18S
HBV RNAs / rRNA 18S
density (ratio)

Figure 7.

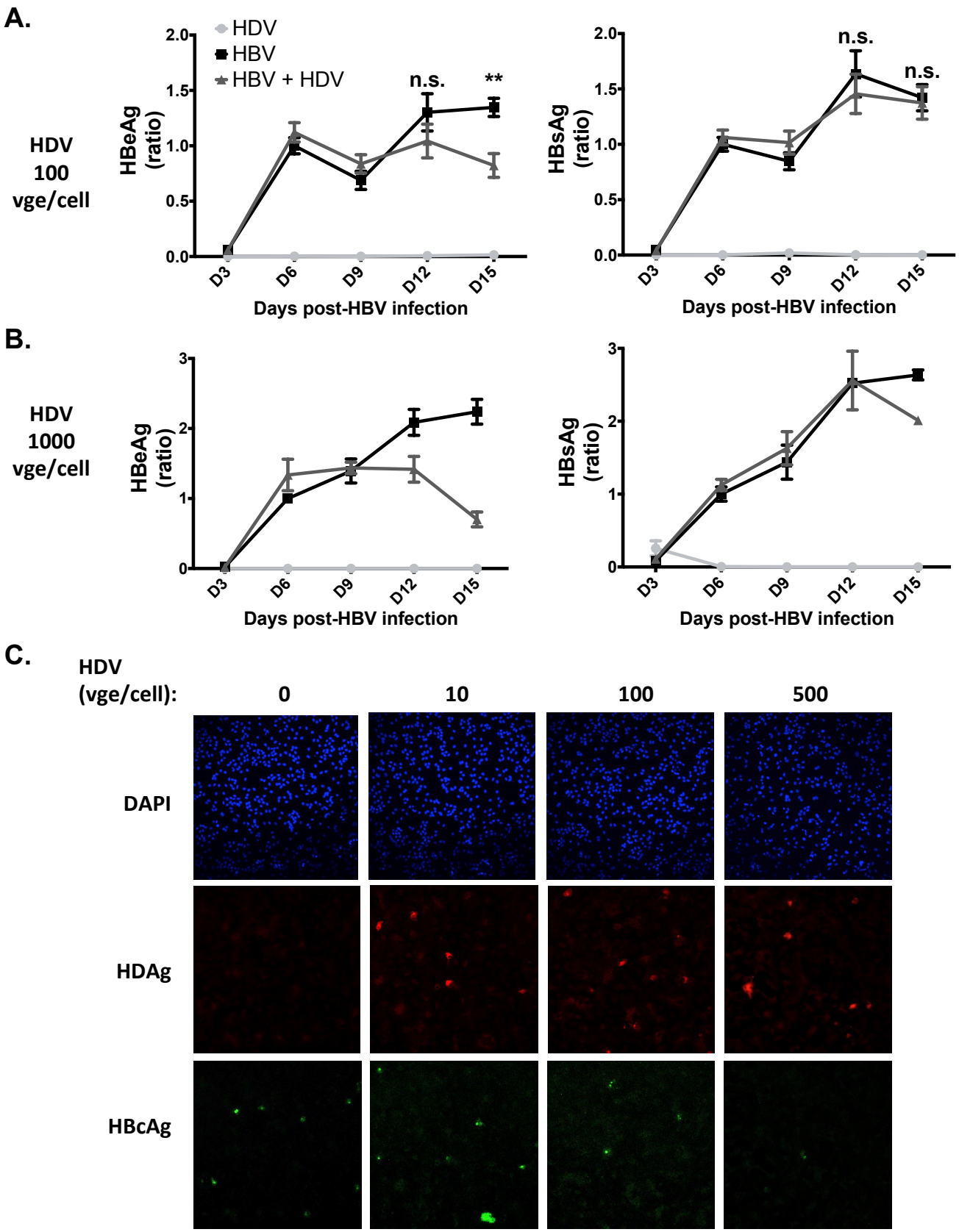
A.
HDV
100
vge/cell
HDV
HBV
HBV + HDV
HBeAg (ratio)
HBsAg (ratio)
n.s.
**
n.s.
n.s.
D3
D6
D9
D12
D15
Days post-HBV infection
B.
HDV
1000
vge/cell
HBeAg (ratio)
HBsAg (ratio)
Days post-HBV infection
C.
HDV (vge/cell):
0
10
100
500
DAPI
HDAg
HBcAg

Figure 8.

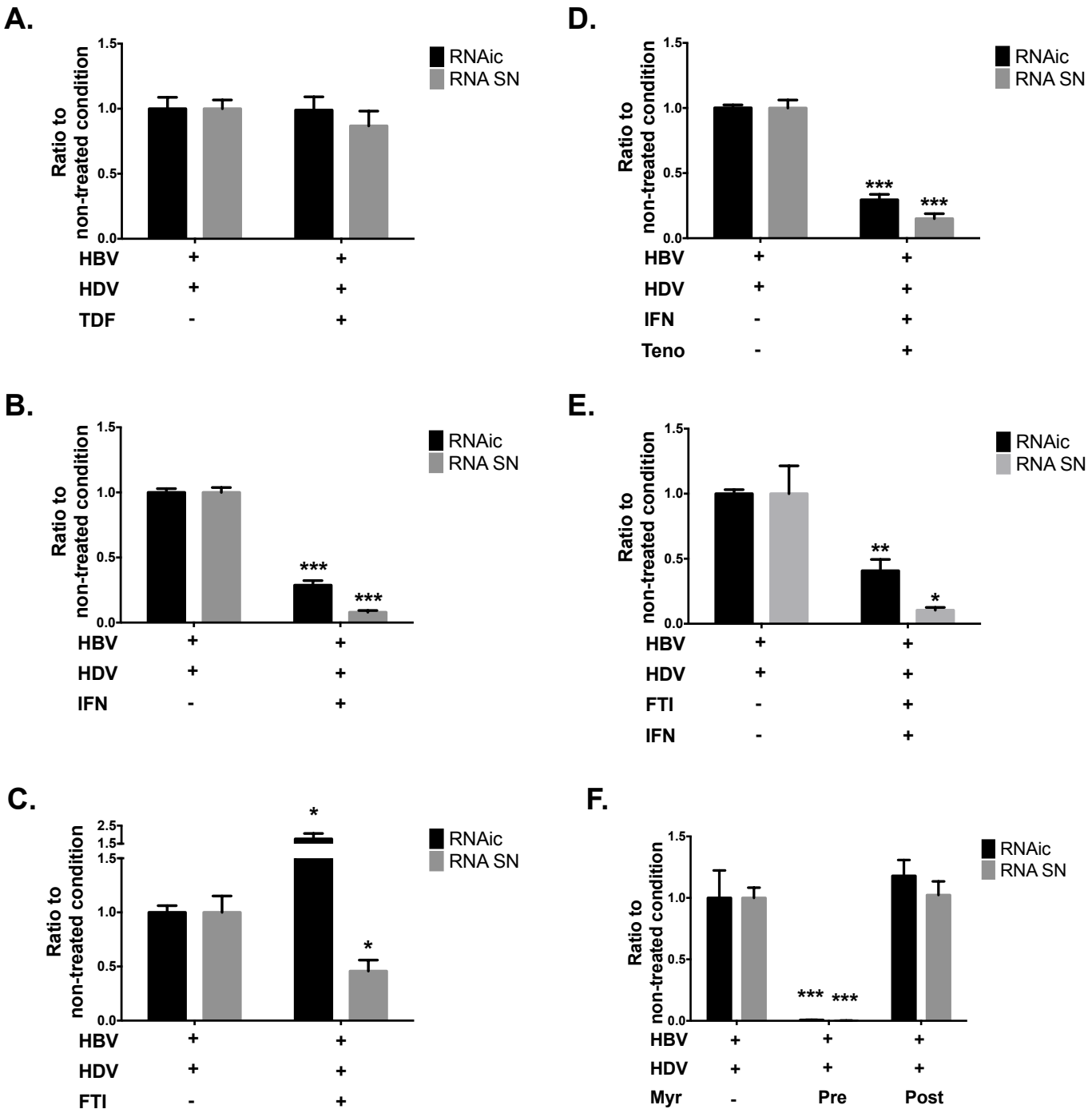
A.
Ratio to non-treated condition
1.5
1.0
0.5
0.0
RNAic
RNA SN
HBV + +
HDV + +
TDF - +
B.
Ratio to non-treated condition
***
***
RNAic
RNA SN
HBV + +
HDV + +
IFN - +
C.
Ratio to non-treated condition
2.5
1.5
*
*
RNAic
RNA SN
HBV + +
HDV + +
FTI - +
D.
Ratio to non-treated condition
***
***
RNAic
RNA SN
HBV + +
HDV + +
IFN - +
Teno - +
E.
Ratio to non-treated condition
**
*
RNAic
RNA SN
HBV + +
HDV + +
FTI - +
IFN - +
F.
Ratio to non-treated condition
***
***
RNAic
RNA SN
HBV + + +
HDV + + +
Myr - Pre Post

Supplementary table and figures

Designation		Sequence (5'-3')
HDV	Forward Primer	CGGGCCGGCTACTCTTCT
	Reverse Primer	AAGGAAGGCCCTCGAGAACA
HBV total	Forward Primer	GCT GAC GCA ACC CCC ACT
	Reverse Primer	AGG AGT TCC GCA GTA TGG
HBV pgRNA	Forward Primer	GGA GTG TGG ATT CGC ACT CCT
	Reverse Primer	AGA TTG AGA TCT TCT GCG AC
HBV cccDNA	Forward Primer	CTC CCC GTC TGT GCC TTC T
	Reverse Primer	GCC CCA AAG CCA CCC AAG
	Probe	GTT CAC GGT GGT CTC CAT GCA ACG T
	Probe	AGG TGA AGC GAA GTG CAC ACG GAC C
GUS	Forward Primer	CGTGGTTGGAGAGCTCATTTGGAA
	Reverse Primer	ATTCCCCAGCACTCTCGTCGG
RPLP0	Forward Primer	CAC CAT TGA AAT CCT GAG TGA TGT
	Reverse Primer	TGA CCA GCC CAA AGG AGA AG
B-globin	Forward Primer	ACA CAA CTG TGT TCA CTA GC
	Reverse Primer	CAA CTT CAT CCA CGT TCA CC
	Probe	CAA ACA GAC ACC ATG GTG CAC CTG ACT CCT GAG GA
	Probe	AAG TCT GCC GTT ACT GCC CTG TGG GGC AA
IL6	Forward Primer	ACCCCTGACCCAACCACAAAT
	Reverse Primer	AGCTGCGCAGAATGAGATGAGTT
IFNa	Forward Primer	GTGAGGAAATACTTCCAAAGAATCAC
	Reverse Primer	TCTCATGATTTCTGCTCTGACAA
IFNb	Forward Primer	GCCGCATTGACCATGTATGAGA
	Reverse Primer	GAGATCTTCAGTTTCGGAGGTAAC
OAS1	Forward Primer	AGGTGGTAAAGGGTGGCTCC
	Reverse Primer	ACAACCAGGTCAGCGTCAGAT
ISG15	Forward Primer	ATGGGCTGGGACCTGACG
	Reverse Primer	GCCAATCTTCTGGGTGATCTG
MxA	Forward Primer	GGTGGTCCCCAGTAATGTGG
	Reverse Primer	CGTCAAGATTCCGATGGTCCT
RSAD2	Forward Primer	CTTTGTGCTGCCCCTTGAG
	Reverse Primer	TCCATACCAGCTTCCTTAAGCAA
RIG-I	Forward Primer	GCTGATGAAGGCATTGACATTG
	Reverse Primer	CAGCATTACTAGTCAGAAGGAAGCA
MDA5	Forward Primer	CCCATGACACAGAATGAACAAAA
	Reverse Primer	CGAGACCATAACGGATAACAATGT

Table S1. List of primers and probes used for qPCR

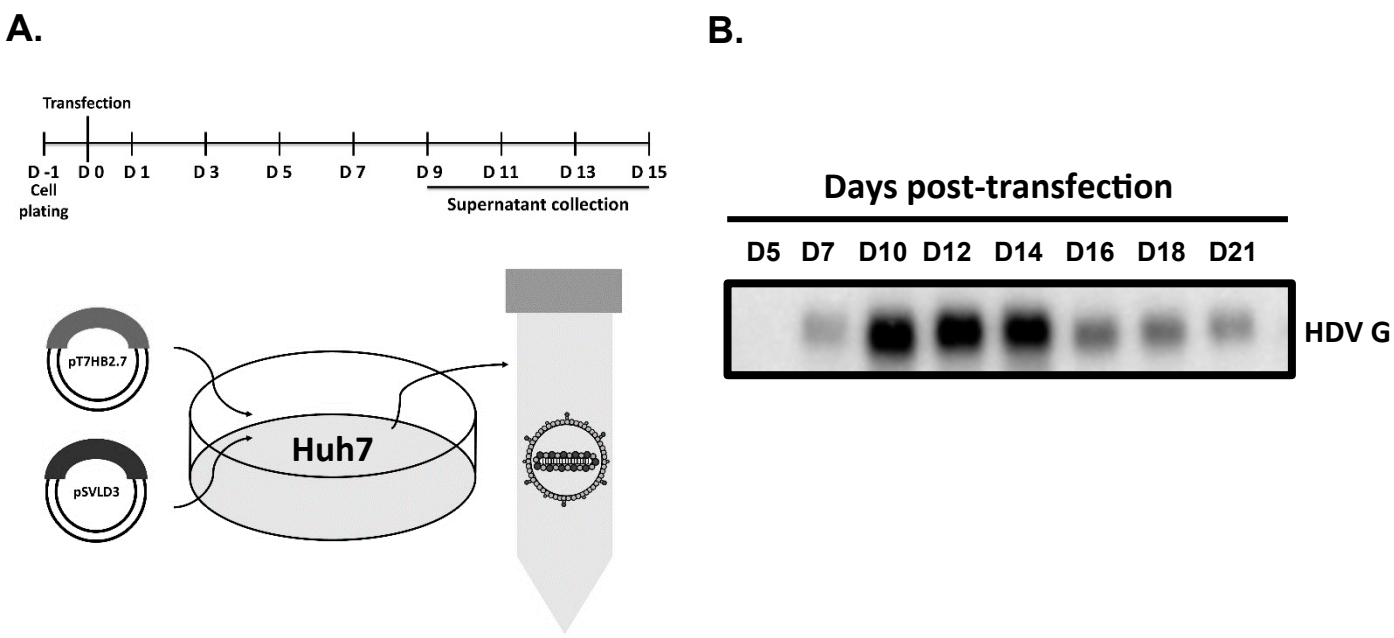

Figure S1. **HDV viral inoculums production**. (A) HDV was produced in vitro by co-transfection of Huh7 cells with T7HB2.7 (coding for PreS1-PreS2-S from HBV) and pSVLD3 (containing a trimer of HDV genotype 1 genome). Supernatant was collected every other day from day-9 to day-15 post-transfection. (B) Northern blot analysis (with a full-length anti-genomic probe, for detection of HDV genome) of HDV RNA in the supernatant of transfected cells throughout time. G, genome.

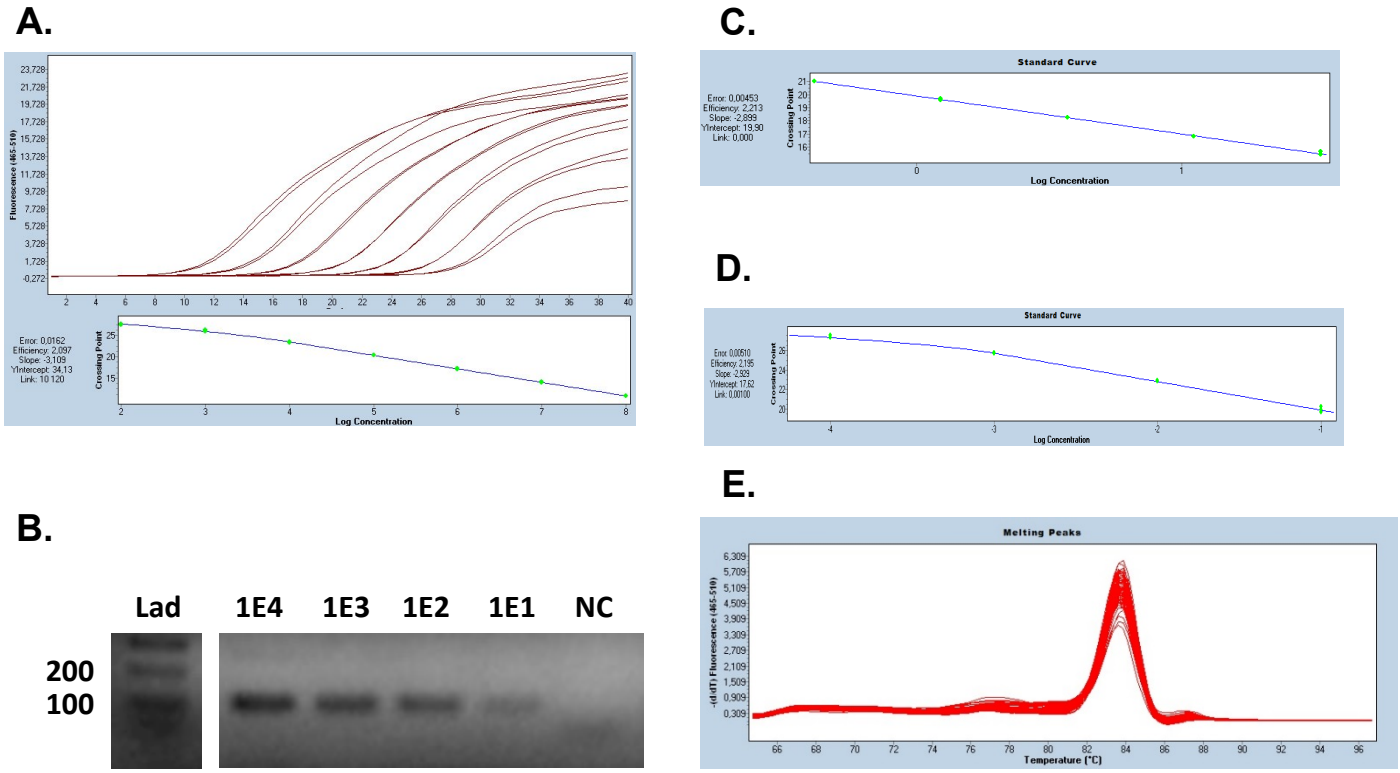

Figure S2. Set up of the HDV RT-qPCR. (A) Serial 10-fold dilutions of a full-length HDV-1 RNA genomic transcript are used as a quantification standard, confirm PCR linearity within a range of 102 to 108 copies/ reaction with a PCR efficiency of ~2,1. (B) Electrophoresis of PCR products evidences a unique band located between 100 and 200bp, consistent with the predicted 129bp amplicon. (C) Serial 10-fold dilutions of RNA extracted from cell culture supernatant, confirm PCR linearity between 6X101 and 6X105 copies/ reaction,with a PCR efficiency of ~2,2. (D) Serial 3-fold dilutions of intracellular total RNA confirm a linear HDV amplification within a range of 0.4-33,3 ng of total RNA per PCR reaction. (E) Melting curve plot of HDV infected samples, confirming one single Tm peak consistently found at 84ºC. Lad, DNA ladder (100bp, New England Biolabs); NC, negative control; Tm, melting temperature.

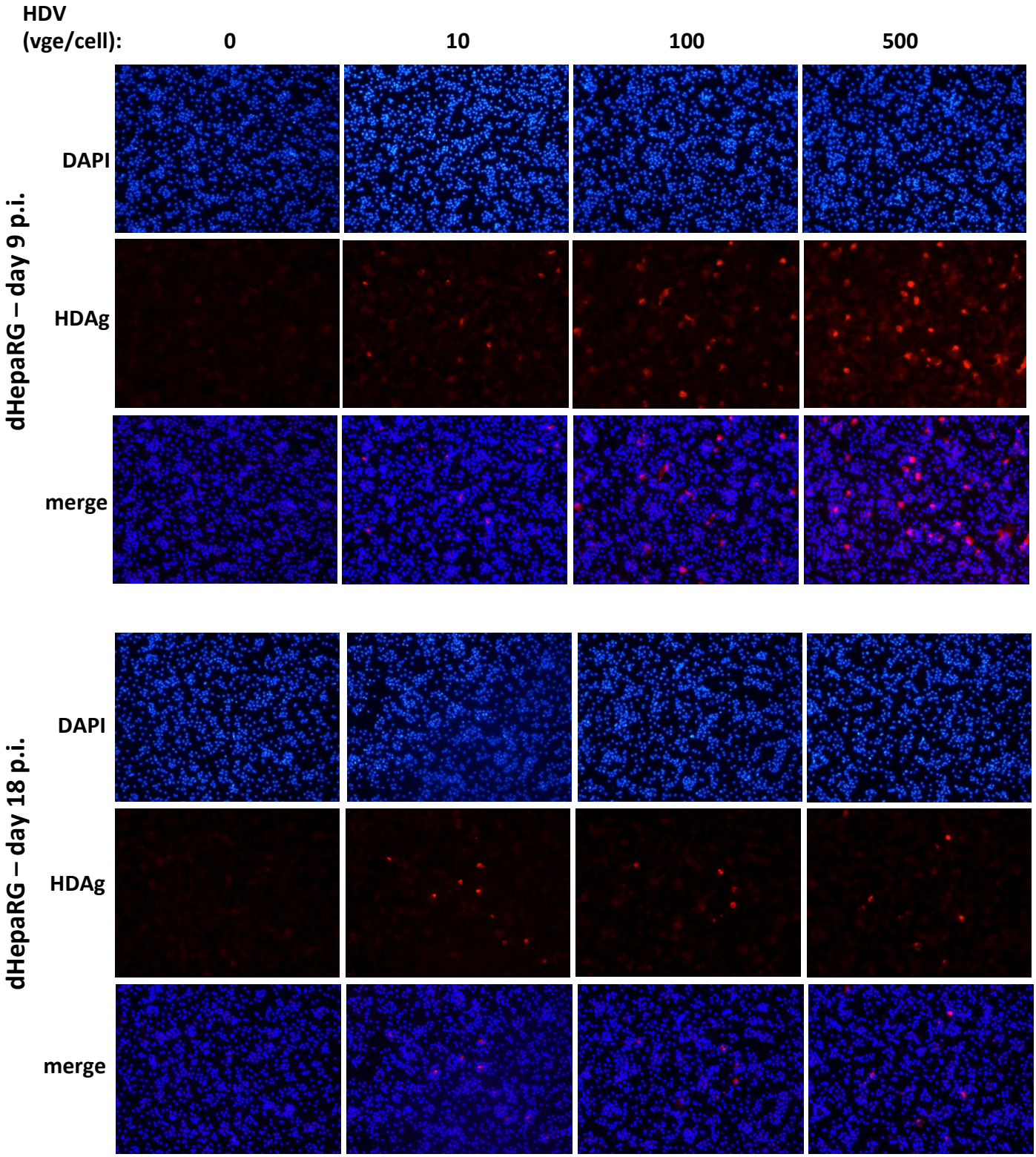

Figure S3. **Increasing MOI lead to increases of HDV infected dHepaRG**. dHepaRG cells were infected by HDV at the indicated MOI. At the indicated time, cells were fixed, permeabilized, labeled with anti-HDAg antibodies and analyzed by epifluorecence microscopy.

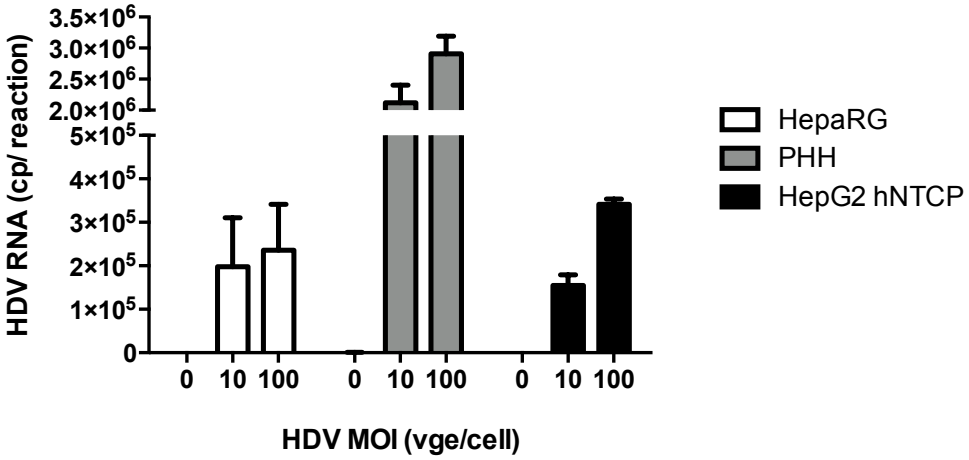

Figure S4. **HDV infection of different cells**. dHepaRG, PHH or HepG2-NTCP cells were infected by HDV at 10 vge/mL. 6 days later, levels of intracellular HDV RNA were assessed by RT-qPCR

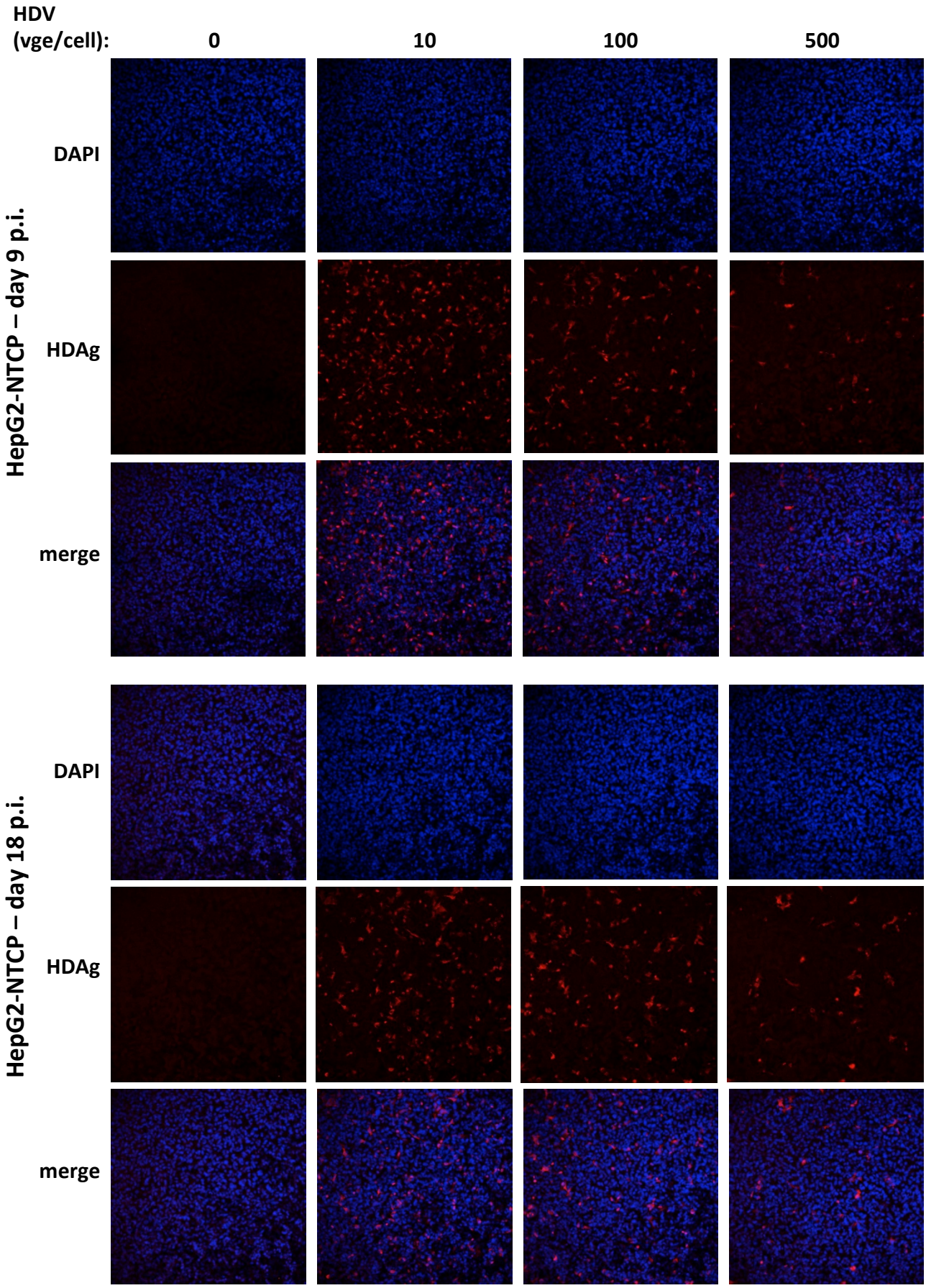

Figure S5. **HDV infection of different cells**. HepG2-NTCP cells were infected by HDV at the indicated MOI. At the indicated time, cells were fixed, permeabilized and labeled with anti-HDAg antibodies and analyzed by confocal microscopy.

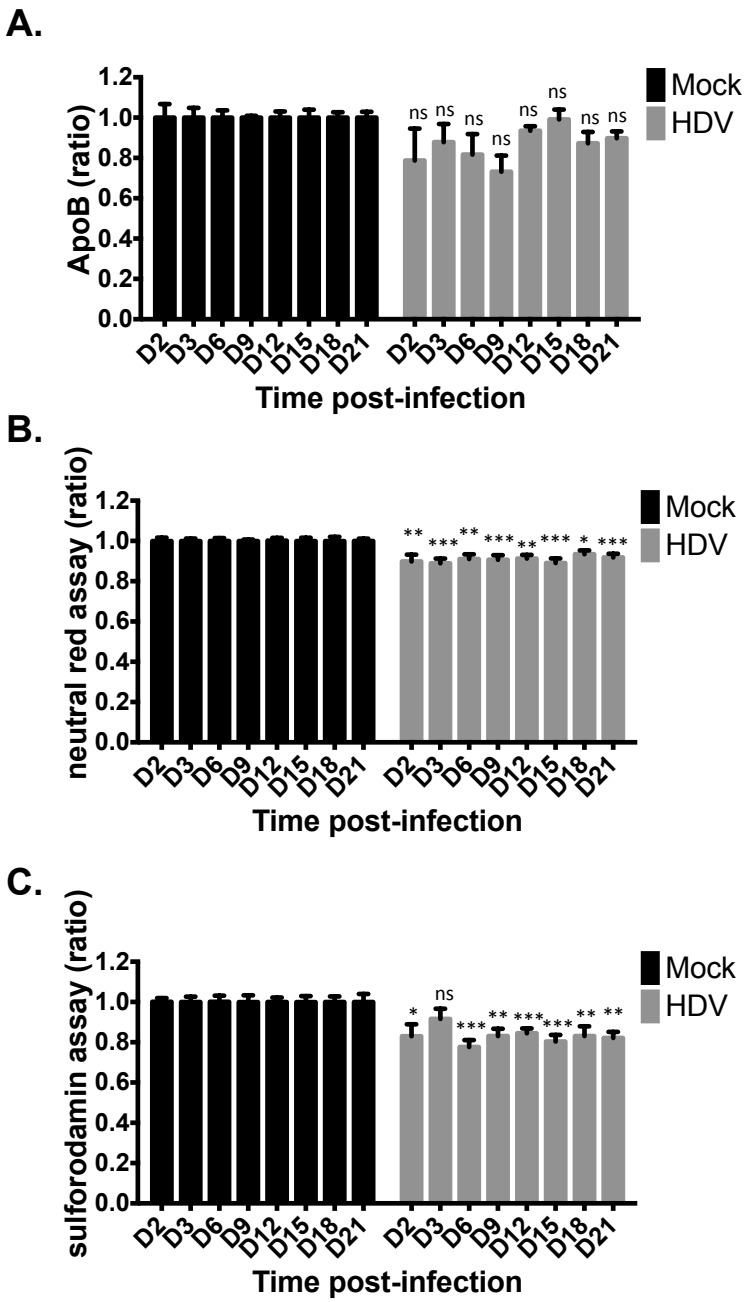

Figure S6. **HDV does not induce specific death of infected dHepaRG cells**. (**A, B, C**) dHepaRG cells were infected with HDV at 10 vge/cell and (**A**) Apolipoprotein B secretion as well as (**B, C**) cells viability were assessed by ELISA, neutral red or sulforodamin assays. Results are presented as ratio to non infected cells (mock) and represent the mean +/-SEM of 8 replicates (**D**) dHepaRG were treated with the indicated concentration of staurosporine and QVD-OPH for 16 hours and ALT activity were measured with colorimetric assays. (**E**) dHepaRG cells were infected by HDV and treated with QVD-OPH for 12 day. Levels of intracellular HDV RNA were assessed by RT-qPCR. Results are presented as ratio to the mock condition and represent the mean +/- SEM of 3 independent experiments each performed in triplicate.

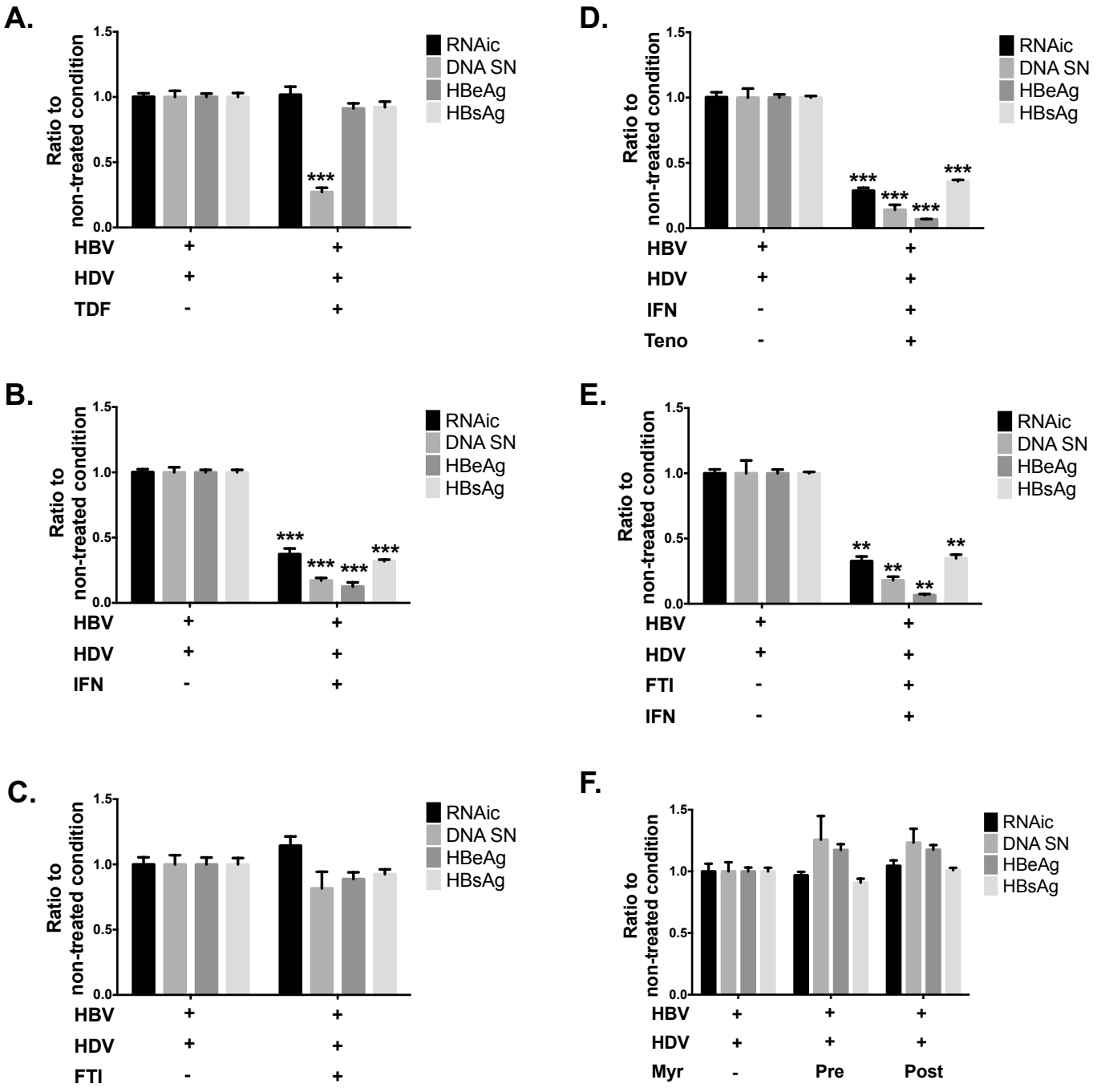

Figure S7. Evaluation of the anti-HBV effect of approved and investigational molecules. dHepaRG cells were infected with HBV at 100 vge/cell for 6 days and super-infected with HDV at the indicated at 10 vge/mL. Three days post HDV infection, cells were treated with (**A**) Tenofovir, (**B**) IFNa, (**C**) FTI-277, (**D**) Tenofovir and IFNa, (**E**) FTI-277 and IFNa for 10 days. (**F**) Cells were treated with Myrcludex B (Myr) either 2 hours before and during HDV inoculation (Pre) or once the infection was established as described for the other drugs. Levels of intracellular HBV RNA (RNAic) or secreted HBV DNA (DNA SN) were respectively assessed by qRT-PCR and qPCR. HBeAg and HBsAg secretion were assessed by ELISA. Results are presented as ratio to the non treated condition and represent the mean +/- SEM of at least 3 independent experiments performed in triplicate.

Figure S8.

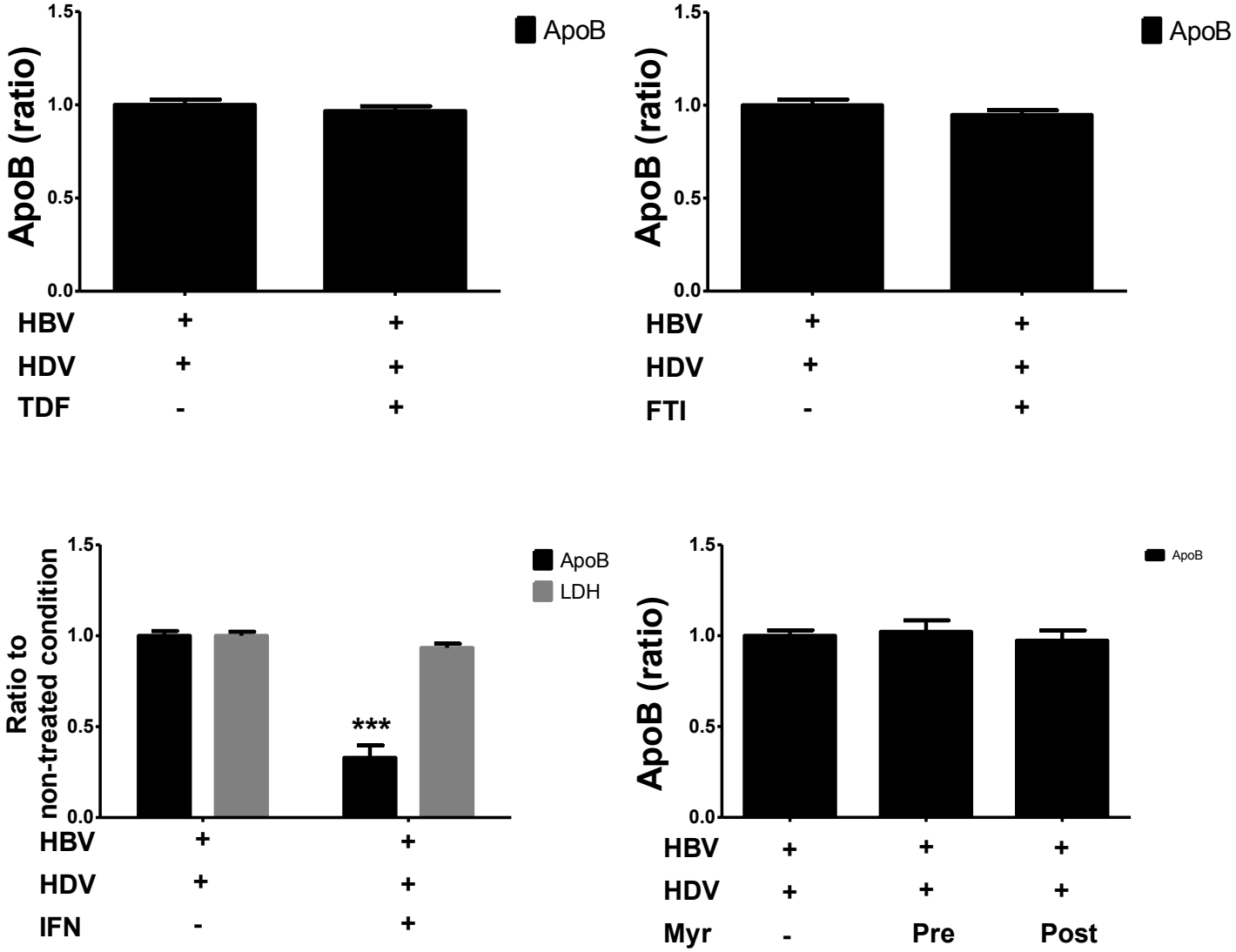

Figure S8. Evaluation of cell viability. dHepaRG cells were infected with HBV at 100 vge/cell for 6 days and super-infected with HDV at the indicated at 10 vge/mL. Three days post HDV infection, cells were treated with Tenofovir, IFNa or FTI-277 for 10 days. Cells were also treated with Myrcludex B (Myr) either 2 hours before and during HDV inoculation (Pre) or once the infection was established as described for the other drugs. Levels of secreted ApoB were assessed by ELISA. When a decrease was identified, lactate desidrogenase (LDH) activity was measured. Results are presented as ratio to the non treated condition and represent the mean +/- SEM of 3 independent experiments performed in triplicate. TDF, tenofovir; IFN, interferon; Myr,myrclydex; Pre, treatment before and during inoculation; post, treatment after infection.

- A model of super-infection with HDV on HBV-infected hepatocytes was established;
- HDV infection induces a strong IFN response in these immune-competent hepatocytes;
- In this model, HDV infection is associated with HBV inhibition, thus access to recapitulating *in vivo* viral interference;
- This super infection model is also suitable for the evaluation of novel drugs/antivirals, including immune-modulators.